CO_2 capturing natural fibre reinforced algae-derived polyurethane composites

Shaping Matter Lab
Sowrabh R. Shetty

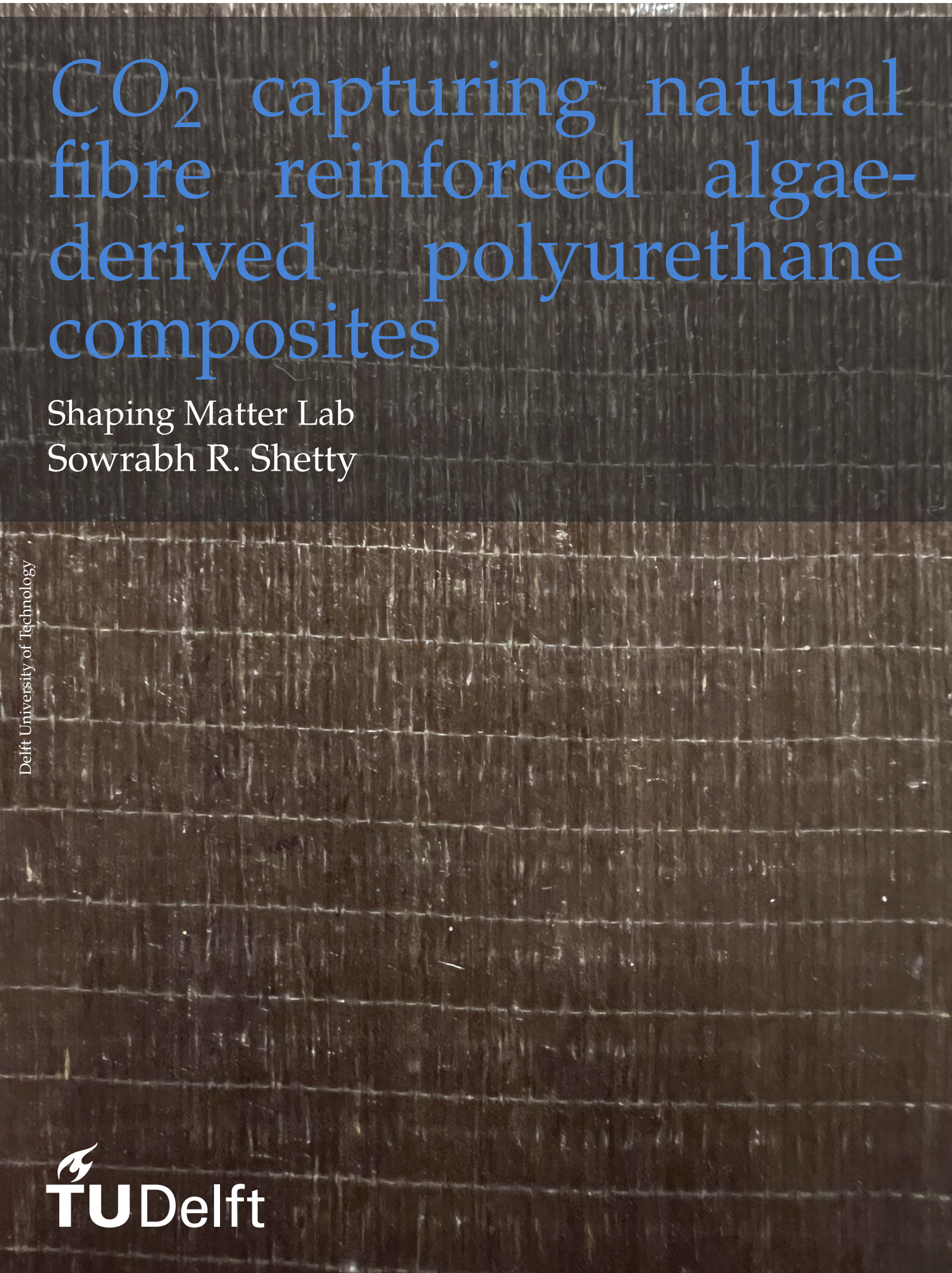

Delft University of Technology

TU Delft

CO_2 capturing natural fibre reinforced algae-derived polyurethane composites

by

Sowrabh R. Shetty

Student Name	Student Number
Sowrabh R. Shetty	5332087

Supervisor:	Dr. Kunal Masania
Daily Supervisor:	Dr. Baris Kumru
Project Duration:	February, 2022 - December 2022
Faculty:	Faculty of Aerospace Engineering, Delft

Style: TU Delft Report Style, with modifications by Daan Zwaneveld

TU Delft

Abstract

In the past two decades, there has been a substantial increase in the use of natural fibres in bio-composites; these fibres have a Greenhouse gas (GHG) footprint of about 60,000 times less than virgin carbon fibres. The synthesis of polymers from renewable resources is gaining importance as a solution to the critical issues of depleting crude oil reserves and widespread pollution. To date, polymers have been manufactured utilising a vast array of biomass and bio-based platform chemicals. One such polymer is Polyurethaneane. Polyurethane (PU) is typically produced through the reaction of a polyol (polyol polyether or polyol polyester) derived from petroleum with isocyanate. With a few adjustments to the polyols and diisocyanates, the properties of PU can be significantly improved. Due to its adaptability, PU is utilised in many products, such as foam, spandex, coatings, and adhesives. Despite its usefulness, the primary raw material of Polyurethaneane (PU) is petroleum-based material which is nonrenewable and has low biodegradability, resulting in severe environmental problems. Cellulose, vegetable oil, lignin, proteins and starches are all biological components that can be used in the synthesis of Polyurethaneane (PU). These biomass materials are advantageous because they are abundant, inexpensive, high-yielding, and have a minimal environmental impact. The primary focus of this study is new developments in synthesising polyols from biomass and their use in PU materials. The primary goal of this research is to characterise a PU produced from algae biomass and utilise this to manufacture a prototype composite material. Whilst also studying the amount of carbon dioxide embodied in the system. The thesis aims to conclude that bio-based resin systems can produce good mechanical properties while reducing environmental impact.

Contents

List of Figures

List of Tables

Nomenclature

Abbreviations

Abbreviation	Definition
AA	Acetic anhydride
AIL	Acid-insoluble lignin
ANOVA	Analysis of variance
CFRP	Carbon fibre reinforced polymer
CSIR	Council for Scientific and Industrial Research
DKL	De-polymerized Kraft lignin
DSC	Differential scanning calorimetry
DTG	Derivative thermogravimetry
EIA	Environmental impact assessment
EOF	End of life
FRP	Fibre-reinforced plastic
FTIR	Fourier-transform infrared
GFRP	Glass fibre reinforced polymer
GHG	Greenhouse gases
HFRP	hybrid fiber reinforced plastics
IR	Infrared
ISO	International Standards Organization
LCA	Life cycle assessment
LCI	Life Cycle Inventory
LCIA	Life Cycle Impact Assessment
NFC	Natural fibre composite
NIR	Near-infrared
OEM	Original equipment manufacturer
OL	De-polymerized organosolv lignin
PAN	Polyacrylonitrile
PATH	Partnership for Advancing Technology in Housing
PP	Polypropylene
PU	Polyurethane
RIM	Reaction injection molding
SEM	Scanning electron microscope
SFFT	Single fiber fragmentation tests
SIP	Structural insulated panel
SRIM	Structural reaction injection molding
TGA	Thermogravimetric analysis
TPU	Thermoplastic polyurethane
UTM	Universal Testing machine
VARTM	Vacuum assisted resin transfer moulding
WPC	Wood/plastic composite
WPC	wood plastic composites

Symbols

Symbol	Definition	Unit
E	Modulus	[GPa]
E"	Loss modulus	[Pa]
E′	Storage modulus	[Pa]
F	Load	[N]
s"	Deflection	[mm]
s′	Deflection	[mm]
T_g	Glass transition temperature	[° C]
T_m	Melting temperature	[° C]
ρ	Density	[kg/m^3]
σ	Stress	[MPa]
ϵ	Strain	
η	Viscocity	[Pas]

1

Introduction

Natural fibres offer an environmentally friendly alternative to glass and mineral fibres. In the last two decades, many natural fibres have been used in biocomposites, mainly for the automotive industry and as insulation material.

In 2012, the European car industry utilised thirty thousand tonnes of natural fibres, primarily in so-called compression-moulded parts, an increase from the roughly nineteen thousand tonnes used in 2005. As illustrated in Figure 1.2, flax held a fifty percent market share of the thirty thousand metric tonnes of natural fibre composites in 2012. Kenaf fibres, with a market share of 20%, are followed by hemp fibres, with a market share of 12%, and other natural fibres, primarily jute, coir, sisal, and abaca, account for 18% ([7]).

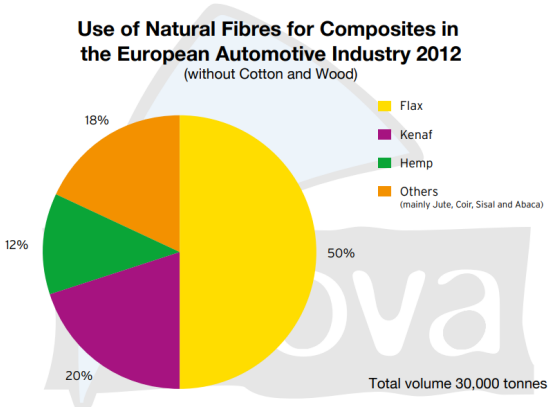

Figure 1.1: Natural fibre composites utilised in the European automobile industry in 2012 (total volume of 30,000 tonnes, excluding cotton and wood); "others" primarily includes jute, coir, sisal, and abaca. [39]

In recent years, ecological concerns and global warming have sparked significant interest in using natural resources to manufacture environmentally friendly products and minimise anthropogenic carbon dioxide emissions by all means feasible. Following the Kyoto Protocol, numerous countries have pledged to reduce their combined CO_2, CH_4, and N_2O emissions by 6% below their 1990 levels between 2008 and 2012. Carbon dioxide emissions from the combustion of fossil fuels account for more than 99 percent of all greenhouse gases (GHG). According to the 2000 carbon dioxide fact sheet, North America had a 28.2% share of total global CO_2 emissions (6 billion metric tonnes of carbon equivalent) based on energy-related fossil fuel consumption (Emissions of greenhouse gases in the US). By substituting glass fibre reinforcements in vehicle thermoplastics, natural fibres can minimise not only CO_2 emissions but also nonrenewable resources in the current context [34].

Research institutions are investigating natural fibres as an environmentally beneficial alternative to glass fibres. Most of the researched bast fibres are derived from naturally occurring flax, hemp, and kenaf plants. These fibres are renewable, non-abrasive to processing equipment, and can be burnt for

energy recovery at the end of their life cycle due to their high calorific value. They are also relatively safe to handle and are unlikely to damage the lungs during processing and use.

There is an intriguing comparison [40] between the tensile strength of several natural fibres and reference regenerated cellulose (rayon). The tensile strength of flax and hemp ranges from 600 to 800 MPa, significantly more than other natural fibres. Natural fibres are 40% lighter than glass fibres in terms of density [13], giving them a competitive advantage in-car applications.

In a study by Van Voorn et al. [40], 2001, the mechanical properties of glass and flax fibre sheet moulded composites based on a wet-laid process were compared. It was determined that the stiffness of flax fibre composites is comparable to or even superior to that of glass fibre composites. At the same time, the flexural and tensile strength properties are slightly lower. However, flax fibre composite impact strength is only 3–7 kJ/m2 compared to 40 kJ/m2 for glass fibre composite. Other researchers have found similar similarities by employing the film-stacking technique [13].

In the greenhouse gas emission impact domain, natural fibres produce lower emissions than materials derived from fossil fuels. Example: making and exporting one tonne of continuous filament glass fibre (CFGF) from a factory generates an average of 1,8 tonnes of carbon dioxide equivalent (CO_2 -eq) emissions. Recent information from Ecoinvent 3.4 indicates that the production of one tonne of glass fibre has a carbon dioxide equivalent impact of 2.5 tonnes. The manufacturing of glass fibre has a climate impact that is four-and-a-half times that of the production of natural fibres, which emits between 0.3 and 0.7 tonnes of CO_2 equivalent per tonne of natural fibre. As illustrated in Figure 1.2, several synthetic fibres have much higher emissions. The greenhouse gas (GHG) footprint of virgin carbon fibre is 2,9450 kg CO_2 equivalents, which is approximately 60,000 times greater than the footprint of recovered carbon fibre. As opposed to organic fibres. However, it is essential to note that carbon fibre's greenhouse gas (GHG) footprint is significantly diminished after recycling. When CO_2 absorption is considered, the differences between natural fibre and other fibres become more pronounced. Like natural fibres, synthetic fibres emit carbon into the environment at the end of their life [39].

Further, many researchers have concentrated on polymer chemistries that are closer to equilibrium, such as polyesters and polycarbonates, to create polymers for a future circular economy. These materials offer the potential benefit of lowering greenhouse gas emissions linked to polymer production. They can be made from bio-based raw materials such as agricultural waste or industrial gases like carbon dioxide. 6–10 The synthesis of bio-based monomers and polymers to aid in the shift away from oil-based plastics must be practical and adhere to the principles of green chemistry [6].

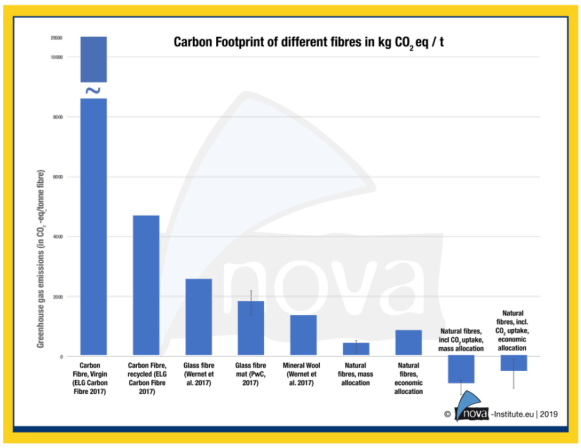

Figure 1.2: Carbon footprint of different materials in kg CO_2 eq/t [39]

This study aimed to explore the mechanical properties and environmental performance of completed natural fibre mat thermoplastic (NMT), which uses a thermoplastic resin with a bio-based origin.

2

Literature Review

Natural composites: An alternative material in engineering

Natural fibre composites are composite materials in which either the fibre or matrix is derived from a biological origin. Fibres are more likely to have a natural origin. They can be used as reinforcements in various forms like long fibres (e.g., bamboo, hemp, flax, jute, sisal, kenaf and ramie), short fibres (e.g., wood fibres, recycled fibres), and fibre fibrils [30]. The matrix can also have a biological origin; Wool et al. discuss biomaterials such as various epoxidised plant oils and soy protein. Nevertheless, most of the NFC are currently prepared with a combination of natural fibres and polymeric matrices derived from petrochemicals [22].

2.1. Natural Fibres

In NFC, the natural fibres are considered the main constituent, as they are the independent constituent of the composite. Natural fibres are classified into three groups based on their origin: mineral, animal and plant. Plant fibres are the most analysed and worked on by the research community. The growth period for these fibres is short whilst also being available abundantly and renewable. The plant fibres comprise cellulose, hemicellulose and lignin [33]. However, in this study, the term natural fibres are directed only to lignocellulosic (plant) fibres.

Hierarchical Structure of a natural fibre

The hollow cellulose fibrils in the plant fibres are held together by the lignin as a binder in the hemicellulose matrix, hence being considered a composite. The unique fibre characteristics of various plants are in the cell wall of the plant fibre as it is inhomogeneous. Multiple layers make up the complicated structure of the fibres. A secondary wall surrounds the thin primary wall throughout cell growth. The secondary wall comprises three layers, S1 (outer layer), S2 (middle layer) and S3 (inner layer). S2 is the most critical layer, as its thickness is essential in determining the mechanical properties of the fibre. The middle layer is complex and comprises helical cellular microfibrils between 10 and 30 nm in length. Microfibrillar angle influences the quality of fibres (smoothness and dexterity). The angle between the axis of the fibre and the microfibrils in the microfibrils angle. The amorphous matrix in the cell wall comprises lignin, pectin and hemicellulose. The hemicellulose molecule is hydrogen-bonded to cellulose and performs as cementing matrix between the cellulose microfibrils to build the fibre cell's main structural element, called the cellulose-hemicellulose network. The primary aim of the pectin and lignin elements is to improve the stiffness of the cellulose/hemicellulose element. An illustration of a natural fibre is shown in Figure 2.1[32]. Moreover, the basic chemical structure of cellulose in all plant-based fibres is similar. However, they have different degrees of polymerisation, whereas the cell geometry of each type of cellulose varies with the fibres. These factors contribute to the various properties of the green fibre Figure 2.2 [16].

Natural fibres have various advantages over synthetic fibres like low cost, availability, acceptable modulus-weight ratio, low density, low manufacturing energy consumption, high acoustic damping, low carbon footprint and biodegradability. However, natural fibres have a few drawbacks due to their low consistency of properties and quality. The fibres have higher moisture absorption, higher physical and mechanical properties variability, lower strength, lower durability, and lower processing temperature.

These variations in the properties are primarily due to the plant, method of fibre extraction, and growth conditions [33].

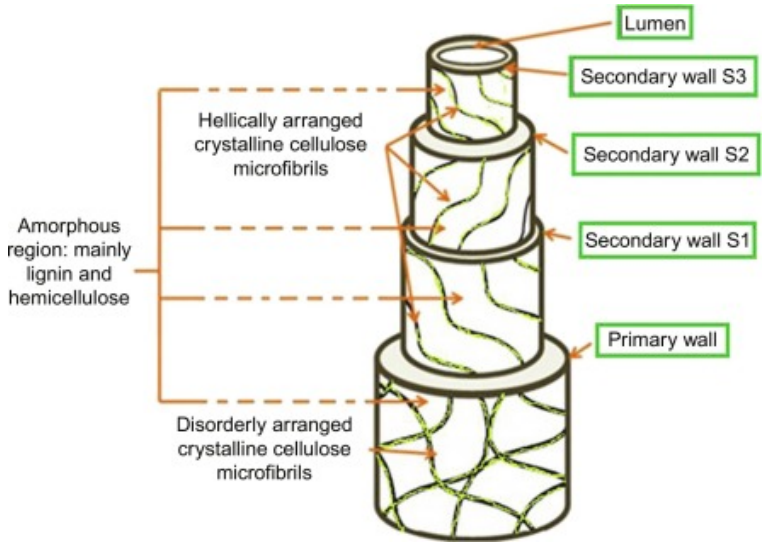

Figure 2.1: Structure of natural fibre separated into various cell walls. Each cell wall displays what is comprises of[32]

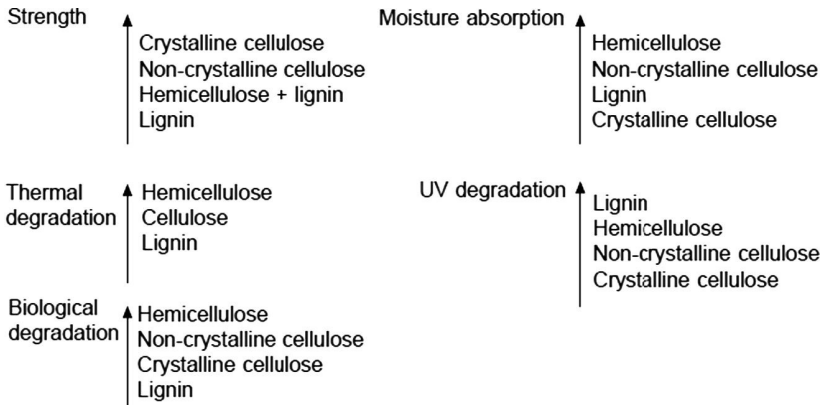

Figure 2.2: Properties of cellulose fibres and their dependence on chemical constituents [16]

The microstructure of natural flax fibres are discussed in detail and as follows:

2.1.1. Flax

Flax *(Linum usitatissimum)* is one of the most widely utilised bio-fibres. A primary reason for this is the stiffness of flax fibres comparable to that of glass fibres, despite having a nearly two times lower density. Flax fibres are produced in the stems of the flax bast plant. Similar to cotton, flax fibre is a cellulose polymer. However, they are more crystalline, making them stiffer, more robust, and crisper to handle. An illustration of the multi-scale structures of flax from stem to the cellulosic fibrils is given in Figure 2.3. The flax plant consists of strong fibres in its stem, which have a diameter of 12-16μm, and can grow to a length of 90cm. The flax stem comprises a xylem, phloem, bark and a central void at a macroscopic level. At a mesoscopic level, 10-40 fibres make up a bundle when they are bound together with the help of pectin. Due to the various materials present in irregular proportions and hierarchical organisation at different length scales, the microstructure of flax fibre is exceptionally complex. At the microscopic scale, each elementary fibre is made of concentric cell walls, which differ in terms of thickness and arrangement of their constitutive components. Lumen contributes to water uptake and is at the centre of the elementary fibre. The secondary cell wall encloses the lumen and is also responsible for the fibre's strength, which is coated by the primary cell wall, which is 0.2μm thick. Every layer comprises cellulose

microfibrils running parallel to each other, forming a microfibrillar angle with the fibre direction. As seen in Figure 2.4, the bulk of the fibres is composed in layer S2 of the secondary cell wall. The S2 layer also includes numerous amorphous hemicellulose and crystalline cellulose microfibrils, oriented at 10 to the fibre axis and giving fibre its high tensile strength. Moving to the nano-scale, an amorphous matrix consisting of hemicellulose and pectin embeds the microfibril's cellulose chains. The microfibril act as the reinforcement within the flax and accounts for about 70% of the weight of the flax fibre. Therefore, the angle between the fibrils and the fibre axis is an essential parameter in depicting the strength of the fibre. Ideally, micro-fibrils with a spiral orientation are more ductile [42].

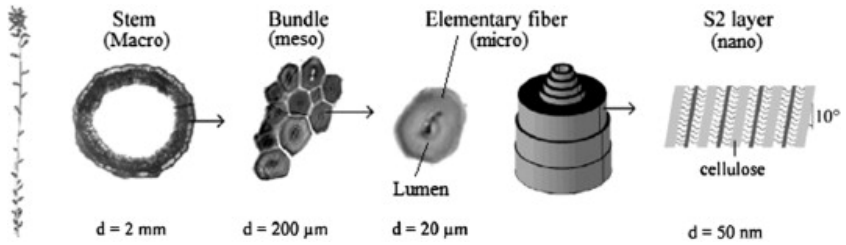

Figure 2.3: Flax structure from the stem to the cellulosic fibrils [42]

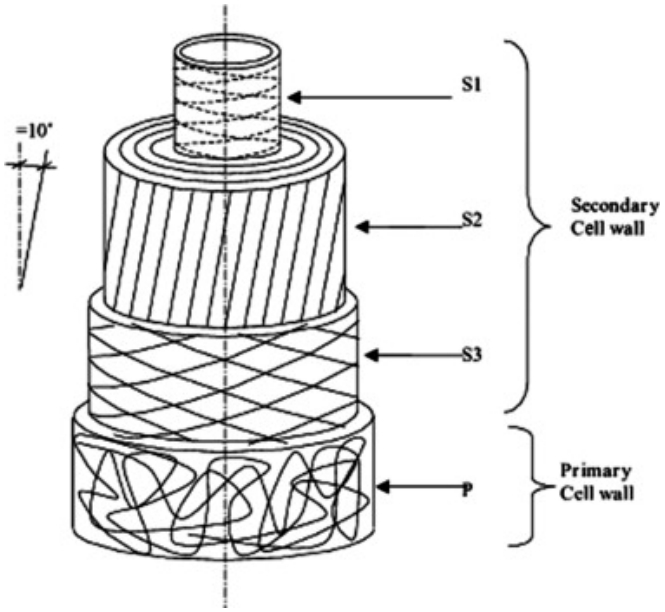

Figure 2.4: The micro-structure of a flax fibre cell [42]

Studies with Flax fibres

Marc Li Loong et al. developed an Acetic anhydride (AA) chemical treatment for unidirectional flax fibre mats to improve composite properties using a bio-resin epoxy in this work. The concentration of the acetic anhydride treatment affected the bio-resin composites. The best tensile strengths and modulus were achieved by soaking flax fibres in 2% acetic anhydride for 1 hour and mixing them with the bio-resin. The lap-splice length and adhesive bond strength were determined using single lap-splice testing. For untreated and chemically treated single-strand flax yarns, the Single fibre fragmentation tests (SFFT) between the flax fibre and bio-epoxy resin provided comparative fibre/matrix adhesion findings. The fibres treated with 2% acetic anhydride formed fewer fragments than the untreated flax control samples. The tensile data support the results. All the AA-treated samples outperformed the untreated fibres regarding moisture differences. Compared to non-treated flax fibres, the fibres treated with 1–2% acetic anhydride were the most successful, with an average moisture resistance improvement of 65%. Scanning electron microscope (SEM) demonstrated that a 2% AA treatment removed the majority of surface waxy compounds. However, a 3% AA treatment caused fibrillation. Reduced fibre

pull-out and tearing of shorter fibres were observed on Scanning electron microscope (SEM) shattered surfaces of AA treated flax fibre composites, indicating enhanced interfacial adhesion. The chemical treatments on flax fibre mats combined into a bio-resin had substantial statistical changes in tensile strength, tensile modulus, and bond shear strength, according to statistical analysis using Analysis of variance (ANOVA). As a result, the treatments influenced the mechanical properties of flax fibres and composites [27].

The mechanical characteristics and durability of flax/glass fibre bio-hybrid fibre reinforced plastics (bio-HFRP) composite laminates were explored in a new study by ZhengyiLiu et al. The mechanical properties of the bio-HFRP composites are significantly improved by glass fibre mixing. Pure flax fibre composites have superior bending and shear characteristics. The layup procedure has a considerable impact on the material's mechanical properties. Sandwich layup composites have higher flexural strength than other layups. G_2F_2s (different stacking sequences G_2F_2, F_2G_2s,F_2G_2s,FG_2Fs,GF_2Gs,F_8 &) has a flexural strength of 358.5 MPa and has the best bending and shear performance after hygrothermal ageing. Furthermore, high-strength glass fibre is used on the tensile side of the outermost layer, which increases the material's bending ability. The inclusion of glass fibres considerably improved the thermodynamic properties of bio- HFRP composites. Moreover, when the sandwich layup method is used, and the outer layer material is glass fibre, the thermal stability performance is the best. With a storage modulus E' of 3865 MPa, a glass transition temperature Tg of 78.93 °C, and a damping factor Tanθ of 0.571, the G_2F_2s samples performed the best. Furthermore, Fick's water absorption law model may be used to characterise the water absorption and diffusion laws of bio-HFRP composite in distilled water at various temperatures. Adding a glass fibre layer to bio-HFRP composites could limit moisture absorption. When the same fibre layer is not dispersedly distributed, and the outermost layer is placed with glass fibre, the composites have the lowest water absorption rate under the same mixing ratio. The larger the water absorption of each composite, the higher the distilled water immersion temperature. Finally, problems such as excessive hygroscopicity and low mechanical strength of plant fibres are unavoidable in applying natural fibre composites. Therefore, it is unreasonable to expect natural fibre composites to replace synthetic fibre-based composites. As a result, bio-hybrid composites will be the material of choice. Hybrid fibre composites lower the amount of synthetic fibre that is petrochemically dependent and non-degradable. While boosting environmental friendliness, it achieves low cost, is lightweight, has excellent mechanical qualities and has low moisture absorption sensitivity. As a result, bio-hybrid composites have a great deal of promise and are a viable alternative to non-hybrid synthetic fibre matrix composites [26].

2.2. Lignin

Lignin is the second-most abundant natural polymer on the planet (after cellulose), and it frequently coheres with cellulose and hemicellulose to form the plant's main supporting structure. The global increase in lignin via biosynthesis is estimated to be 61014 t per year. Unfortunately, lignin's complex structure makes it difficult to understand and use. Lignin, on the other hand, is regarded as an excellent biomass chemical raw material and is receiving a lot of attention in the field of materials. This is due to its diverse functional group, renewable nature, degradability, nontoxicity, and low cost (lignin could be produced as a byproduct in the paper industry). Lignin has recently been used in the production of phenol-formaldehyde resin, polyurethane, epoxy resin, and ion exchange resin [19].

Lignin is composed of polyphenolic monolignols or hydroxy cinnamyl alcohols, especially coniferyl alcohol, sinapyl alcohols and p-coumaryl alcohol Figure 2.5, which are in turn synthesised from phenylalanine derived from shikimate biosynthetic pathway. A series of chemical reactions like hydroxylation, deamination, reduction and methylation is used for the biosynthesis of lignin monomers in the cytoplasm. These monomers are transported to the apoplast and polymerised with the three monolignols into plant cell walls by the peroxidase and laccase enzymes. Upon polymerisation, these units are called p-hydroxyphenyl (H) (p-coumaryl alcohol), syringyl (S) (from sinnapyl alcohol), and guaiacyl (G) (from coniferyl alcohol) units [31].

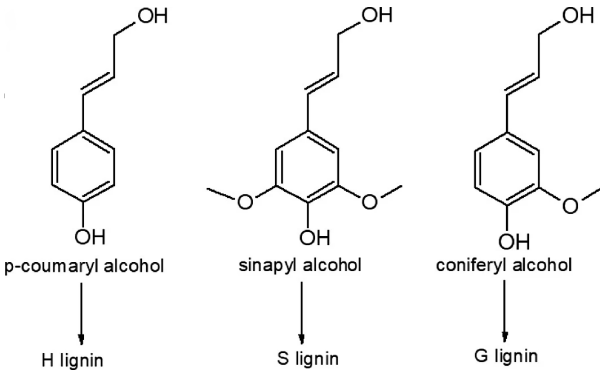

Figure 2.5: Three basic structures of lignin monomers: pcoumaryl alcohol [p-hydroxyphenol (H)], sinapyl alcohol [syringyl (S)] and coniferyl alcohol [guaiacyl (G)] [31]

Variations of the composition of the units are found in different species and taxa of plants. For instance, angiosperm lignin comprises mainly S and G units. However, gymnosperms consist primarily of G units in their lignin with a small number of H units. On the other hand, a high value of H units can be found in grasses. A study by Calvo-Flores et al. stated that about 30% of the total mass in softwood species is lignin, and in hardwood species, lignin amount to about 20-25%. The polymerisation of lignin is catalysed by a peroxidase-mediated dehydrogenation of monolignols, resulting in an optically inactive heterogeneous structure [5]. Degradative methods help better understand the lignin structure's intermolecular meshwork, providing lignin fragments for GC-MS analysis by controlled bond cleavage. Lignin, isolated from different sources, has a molecular mass of 1000–20,000 g/mol. However, determining the degree of polymerisation can be a challenge. This is mainly because the extraction methods fragmentise lignin, randomly yielding various repeated substructures. Nevertheless, two types of lignin structures have been identified based on model studies. Type I lignin contains a glucomannan-lignin-xylan complex directly bonded to cellulose fibrils through hydrogen bridges. In contrast, type II lignin contains xylan-lignin-glucomannan complex embedded thin type I lignin of cellulose fibrils [31].

2.2.1. Role of Lignin

The evolution of lignin structure is thought to have evolved due to plant adaptation to terrestrial life for tall growth. However, marine algae have been found to have lignin and secondary wall structures, demonstrating convergent evolution. Furthermore, numerous biotic and abiotic stresses have been proposed to stimulate lignin production. As a result, it would be reasonable to argue that lignin biosynthesis and biological functions are linked [31]. The fundamental biological function of lignin in plants is explained further below.

Affect on Plant Growth and Development

The most significant function of lignin in plant structure is to provide mechanical strength, water resistance, and protection against microbial destruction of plant cell polysaccharides. However, lignin plays a crucial role in plant growth and development at various stages. According to research, decreased lignin content in seed coats results in lower seed germination rate, slowed development, and fewer seeds. A few studies have also seen apical dominance loss and male sterility. The specific mechanism by which lignin influences plant developmental processes is unknown. However, abnormalities in the cell wall are thought to affect transcriptional processes and signalling pathways, resulting in stunted growth.

Lodging resistance is another crucial element of plant development where lignin has a role. The bending of crops near the ground, which makes them harder to harvest, significantly impacts crop development and output. The effects of lignin deposition on lodging resistance have been examined. Peng et al. investigated the effects of paclobutrazol on lignin deposition and subsequent lodging tolerance in one of the studies. They concluded that the medication boosted lignin deposition and improved wheat lodging tolerance while reducing internode length [4]. Other parameters influencing lignin deposition and lodging resistance include crop density and the activity of lignin production enzymes. Higher nitrogen fertilisers decreased lignin accumulation and reduced lodging resistance, but silicon improves lignin accumulation, and increases stalk length and resistance to lodging [43].

Stress Tolerance and Adaptation

Plant cell wall lignin buildup is also linked to plant resilience to numerous stimuli such as drought, salt, temperature, pathogens, and heavy metals. Drought and salt stress cause osmotic stress, which causes plant death by dehydration. Lignin in the cell wall protects membrane integrity and reduces water loss through transpiration. The amount of lignin in the stem increased under drought circumstances, implying a solid link between lignin biosynthesis genes and drought tolerance.

Temperature is another crucial regulating element in plant development. Extremely high temperatures can destroy proteins, enzymes, and other macromolecules, causing irreparable harm to the plant's metabolic processes. Damage to vascular tissues due to diminished lignin absorption, resulting in excessive transpiration and warming of plant macromolecules, might be one cause. On the other hand, low temperatures may impede plant growth and development by decreasing photosynthesis. In addition, heat and low-temperature conditioning downregulated HSF gene expression, resulting in lower lignification, according to Guy et al. (2007) [15]. Guy et al. (2007) also found that inducing lignin deposition at high temperatures after harvest contributed to environmental stress tolerance in fruit pericarp [15].

Plant heavy metal tolerance is regulated in part by the cell wall. Severe metal stress has increased phenolic material synthesis and lignin content. It has been suggested that lignin, which has numerous functional groups, can bind to heavy metal ions and inhibit their entry into the cytoplasm. Tea plants are known to thrive in soils with high levels of aluminium. Under high aluminium concentrations, the enzymes phenylalanine ammonia-lyase and cell wall peroxidase showed significant reductions, as did the lignin content. This indicates that tea plants are found in areas with high levels of aluminium. Copper and cadmium have also been shown to enhance the amount of lignin in plants. Higher copper concentrations resulted in greater phenolic and lignin accumulation in ginseng due to increased enzymatic activity. In contrast, cadmium treatment increased lignin content upregulation of POD and LAC activity [31].

It has also been suggested that lignin deposition in root endoderm cell walls affects heavy metal transfer into the xylem [25]. For example, lignin biosynthesis genes in Thlaspi caerulescens (Zn/Cd hyperaccumulator) showed increased expression, linked to higher Zn and Cd accumulation. Another vital role lignin plays in plant health improvement is providing pest and disease resistance. Pathogen-infected plants are thought to produce a considerable amount of lignin with a more excellent H unit, which may act as a barrier to pathogen spread and toxin penetration into plant cell walls. In addition, additional lignin-related chemicals may cause them to lose their pathogenicity against the host, resulting in their spread [25]. Specific investigations reveal upregulation of lignin-producing genes in insect-resistant rice infested with brown planthoppers, implying that pest-resistance genes collaborate with lignin-synthesis genes (Jannoey et al., 2017) [21]. Another study found that increasing the expression of lignin genes in chrysanthemums increased the plant's tolerance to aphid assault. Similarly, ethylene-based lignin deposition in the roots boosted the mechanism of action of Sclareol, an antibacterial chemical that promoted root-node nematode resistance in *Arabidopsis thaliana* [31]. The importance of lignin in plants is demonstrated s above. In addition, it is a prominent structural characteristic that is critical for plant growth and development, making it physiologically significant.

2.3. Algae Matrix

This chapter will concentrate on the renewability of a single polymer type, Polyurethane (PU). PU is one of the most versatile artificial polymeric materials, having been discovered by Otto Bayer at IG Farben in 1937. Going into more detail on how to modify biologically obtained precursors to enable applications such as films, coatings, adhesives, sealants, soft foams, rigid foams, elastomers, and hard plastics, by highlighting the diversity of all forms of PU. Because of their exceptional qualities, such as a wide range of hardness, abrasion, and tear resistance; flexibility and elasticity; and bonding ability, PUs have found use in a wide range of commercial items. PUs are also quite affordable to produce. While biobased PUs in specialised applications such as flame retardation and TPU resins are given special consideration, this Review does not focus on structure-property correlations. Furthermore, due to its low cost and excellent availability, the greenhouse gas CO_2 has lately been investigated as a viable polymer feedstock, resulting in a number of environmental benefits and cost savings for use in TPU adhesives and coatings [37].

The development of renewable PUs will be highlighted in the following sections, with an emphasis on individual biosourced precursors. While other researchers have focused on biobased non-isocyanate PUs and other green PU synthetic pathways, this Review focuses solely on precursors rather than PU

synthesis itself. The production of a urethane (or urea) bond is achieved by combining two significant precursors, a polyol and an isocyanate, with the addition of diols, diamines, surfactants, catalysts, and other types of chain-extender cross-linkers. Variation of the polyol side of PUs has been one way to modify the resultant PU attributes. Polyol precursors can have as few as two hydroxyl groups or as many. Polyols for various product variations are available from commercial PU system vendors. Isocyanates are usually difunctional and have a structure that is aromatic, aliphatic, or alicyclic. Due to the intricacy of their manufacture, which often requires phosgenation, only a restricted number of diisocyanates are available commercially [37].

2.3.1. Types of polyurethane

Diisocyanate or polyisocyanate monomers react with a combination of diol, triol, or polyol building blocks to produce PU (Figure 2.6). In some circumstances, difunctional or multifunctional amine molecules are utilised to produce polyurea or PUurea copolymers, either alone or with polyols. So far, no biobased diamine has been documented in the creation of PU, so they are omitted. Polyols are commonly employed to control urethane polymer hardness. The soft segments of polyols are often comprised of oligomeric polyether, polyester, or polycarbonate diols. Other speciality polyols, such as polybutadiene diol, polydimethysiloxanediols, and acrylic polyols, have not been widely used due to their high cost. The hard segment of PU is made by combining a short-chain diol or diamine with diisocyanate, the composition and ratio of the complex and soft segments determining the chemical and physical qualities of the resulting PU product. Although some PU products, such as coatings and adhesives, include a combination of thermoplastic and thermoset composition, commercial PU goods are generally classed as thermoset and thermoplastic. The presence of any trifunctional or multifunctional component results in chemical cross-linking and so generates a thermosetting polymer, whereas PU formed entirely of difunctional components are thermoplastic [37].

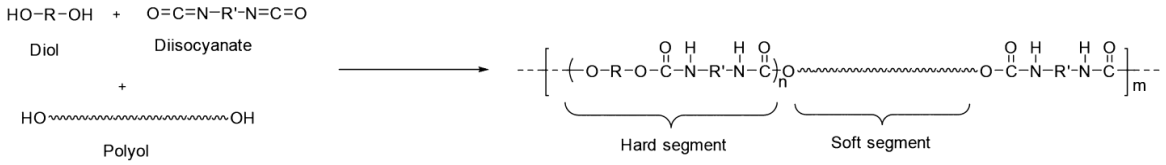

Figure 2.6: Diisocyanate react with a combination of diol, triol, & polyol building blocks to produce PU [37]

Themoset Polyurethane

Chemical cross-linking is abundant in thermoset urethane polymers. This polymer form is only employed in applications that can accommodate polymerization at the production site for end-use due to processing restrictions. The completed polymer materials are primarily employed in mass-market applications such as flexible or rigid foams and rim items. After polymerization, thermoset PU cannot be melt processed, reshaped, or reformed. Thermoset foam products can be cut into various shapes and sizes to suit the application, but they cannot be reprocessed or recycled. Making these polymers biodegradable and employing more biobased raw materials in the production of thermoset urethanes can significantly enhance their environmental effect. In the building business, PU foam materials are widely employed as insulators. Seat cushioning in automobiles and furniture is another prominent application for PU foams. Shoes, helmets, sports and recreation equipment, floor mats, and other industrial and domestic items use thermoset urethanes. However, the market for thermoset urethane is price sensitive due to its large-volume commodity-type applications, and it will most likely resist the adoption of renewable raw materials if they are not cost-competitive with petroleum-based raw materials counterparts [37].

Thermoplastic Polyurethane

TPU are segmented PUs that are meant to be melt-processable and are often delivered as dry TPU resin, solvent-borne urethane solution (SBU), or waterborne PU dispersion (PUD). The dry TPU resin is usually delivered as a pellet, which can then be extruded or moulded into a completed product. The physical performance of thermoplastic urethanes is highly influenced by intermolecular physical crosslinking arising from hard-segment phase separation and crystallisation (Figure 2.7). This is also true for partially crosslinked PU goods, which have a combination of phase separation and chemical crosslinking for

physical strength. The technology of TPU has expanded into a wide variety of applications due to the diversity of chemistry and availability of many building blocks. Shoe soles, wire and cable jackets, hose and tubing, synthetic leather, ski shoes and rollers, protective films and sheets, bullet-proof glass, catheters and balloons, implants, band-aids and dermal patches, golfballs, stretchable fabrics, automotive parts, printed electronics, and many other applications are examples of TPU applications. Coatings, binders, and adhesives all use PU, both solvent-borne and waterborne. Automotive top coats, aerospace, wood floor finish, textiles, furniture and cabinets, and glass coatings are all applications for SBU and PUD coatings. Glass sizing, wood composites, structural sealants and adhesives, electronics, and several other adhesive applications are examples of its use in adhesives and binder applications [37].

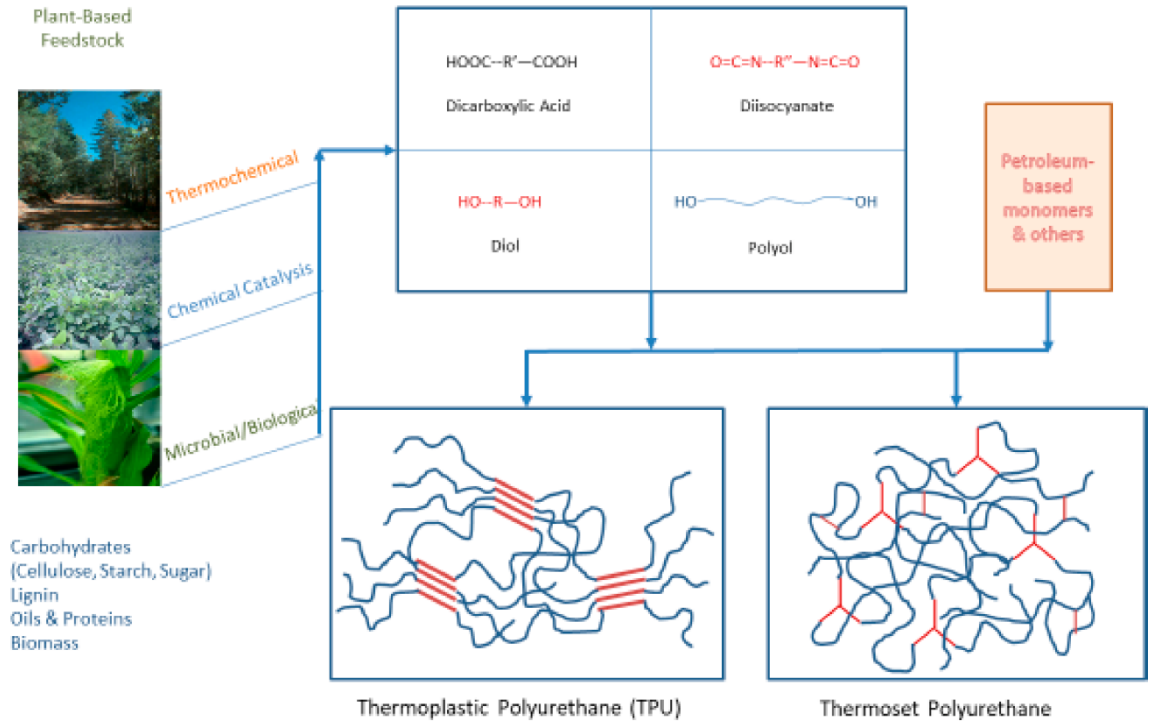

Figure 2.7: Different types of PU resins. The presence of any trifunctional or multifunctional component results in chemical cross-linking and so generates a thermosetting polymer, while thermoplastic PU is formed entirely of difunctional components [37]

2.3.2. Bio based Isocynates

Polyisocyanates, the second component in PU production, are produced industrially by phosgenating primary amines. Because of the toxicity of phosgene, alternative techniques such as Curtius, Hofmann, and Lossen rearrangements are being investigated to replace phosgenation.However, carbonyl nitrene intermediates break down and rearrange to isocyanate in these chemical reaction routes, creating a sudden exothermic peak, which creates a safety risk for large-scale production. Continuous manufacturing has proven to enhance the safety profile for reactions involving nitrogen-to-carbon rearrangements in the last few decades, thanks to tremendous advances in flow chemistry. Continuous flow synthesis can approach a Curtius, Hofmann, and Lossen transformation on a kilogramme scale, allowing for mass production of isocyanates without phosgenation. Petrochemicals are the primary source of aromatic and aliphatic isocyanates. Several biobased polyisocyanates derived from biomass have been explored and developed for years to boost the biobased content in PU formulation. The goal is to increase biocompatibility and biodegradability and replace petroleum-based polymers. Biomass is any organic matter, such as wood, crops, and algae, that absorbs energy from the sun and uses it to transform water and carbon dioxide into oxygen and carbohydrates through a process known as photosynthesis. Converting biomass into various renewable functional molecules (e.g., alcohols, alkenes, acids) can meet the growing demand for environmentally acceptable energy and chemical products. Several recent reviews have examined the chemical conversion pathways from biomass to carbohydrates, including

monosaccharides, disaccharides, and polysaccharides. The most promising carbohydrates-derived platform chemicals are being explored for use in the production of monomers for polymer synthesis. Wood, farm materials, solid waste, and algal sources have been used to synthesise biobased isocyanates. There are seven types of renewable isocyanates: (1) amino acid-based polyisocyanates, (2) sugar-based polyisocyanates, (3) furan-based polyisocyanates, (4) lignin-based polyisocyanates, (5) cashew nut shell liquid-based polyisocyanates, (6) vegetable-based polyisocyanates, and (7) algae-based polyisocyanates, which now allow for the production of sustainable PU with high biobased content [37].

Preparation of Mono- and Diisocyanates in Flow from Renewable Carboxylic Acids

Thien An Phung et al. propose a method to prepare 1,7-heptamethylene diisocyanate (HpMDI, **1**) from azelaic acid (AA, **2**). A nine-carbon diacid is made via ozonolysis from algae-sourced palmitoleic acid. They identified a potential to use the Curtius rearrangement to achieve this transformation, but the stability of the required diacyl azide intermediate was a concern. As a result, they use continuous flow chemistry to mitigate the dangers of unstable reactions or intermediates. Hydrazide chemistry was looked into to prepare acyl azide, where flow methods could provide a realistic answer by allowing for both safety and scalability. They stated that by azidinating the more stable nonanedihydrazide (**3**) with nitrous acid inflow and coupling this to an in-flow Curtius rearrangement, they could make azelaoyl azide (**4**) [36].

To achieve the azelaic acid (**2**) to 1,7-heptamethylene diisocyanate (**1**) transition, azelaic acid was first converted to azelaic dimethyl ester through Fischer esterification, then in situ treated with hydrazine hydrate, and last filtered to extract nonanedihydrazide (**3**). In the first stage of Figure 2.8, batch chemistry was employed to collect (**3**) from (**2**). In continuous flow at 0 °C, the injection of nitrous acid converted intermediate (**3**) to azide (**4**). Following the addition of toluene to the flow, organic soluble (**4**) was extracted into the organic phase using a Zaiput separator. An in-line sodium sulphate column was used to dry (**4**) in toluene, which was then heated in flow at 85° C to trigger the Curtius rearrangement and yield (**1**) in 80 percent at a rate of 500 mgh^{-1}, as shown in Figure 2.9 [36].

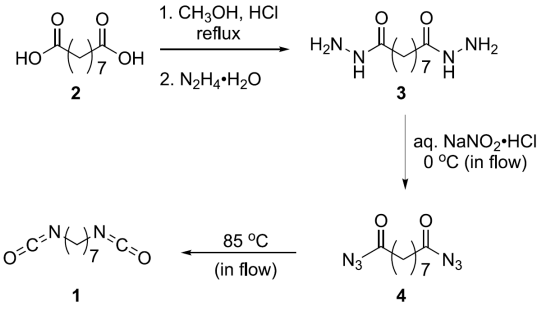

Figure 2.8: Chemical route toward the synthesis of 1,7-heptamethylene diisocyanate (1) from azelaic acid (AA, 2) [36]

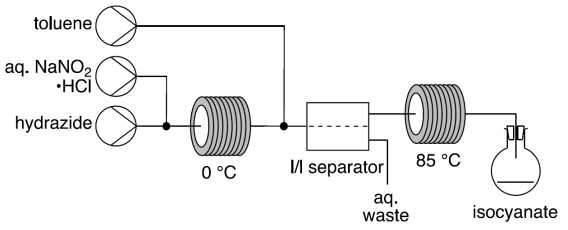

Figure 2.9: Flow chemistry diagram for the synthesis of isocyanates from acyl hydrazide derivatives [36]

2.3.3. Bio based Polyols

Plant growth and oil processing are the key differences between algae and vegetable oil polyols. The most common vegetable oils (such as soy, palm, and rapeseed) were produced in 200 million tonnes per year in 2019 and cost roughly $50000 per tonne as of March 2020, with the majority being used in food goods. Algae may be cultivated on nonarable land and can not compete with food production. However, it is now regarded as a niche commodity and costs nearly twice as much to cultivate and process. Algae growers currently operate in inhospitable environments in Arizona, Hawaii, and Sandia. Algae is also 5 to 44 times more productive than traditional oil-producing plants like corn or soy oil. Depending on the strain and season (if cultivated outdoors), the oil comprises between 30 percent and 80 percent of algal biomass (if cultivated outdoors), which influences productivity metrics. As a result, many algae researchers regard algae oil as a possible windfall if the cost of production can match that of other prevalent plant-based oils, and they are aggressively pursuing technological breakthroughs that will result in algae oil that is less expensive to manufacture. These properties make algal oil attractive for future green technology uses, such as integration into polymers like polyurethane (PU). The only difference between algae oil and other plant-based oils is the fatty acid content. As a result,

the synthesis of algal oil polyols (one of the primary components in PU) is identical to the synthesis of polyols derived from vegetable oils. Traditional procedures such as epoxidation/ring-opening, ozonolysis, hydroformylation, and hydrothermal liquefaction have synthesised polyols from algal oil. However, more research is needed to properly understand algal oil and its potential for PU applications based on the absence of research. Three investigations showed that algal polyols were epoxidised with hydrogen peroxide and ring-opened using HBF4 and methanol, lactic acid, or ethylene glycol. First, triglycerides having secondary alcohol substituents midway down the fatty acid chains at unsaturation locations were generated by ring-opening with methanol. The polyols, which had hydroxyl values of 150 and 317, were utilised to make elastomers and rigid foam insulation samples and were said to be equivalent to petroleum counterparts. With secondary alcohols also present on the lactic acid ester substituent, ring-opening with lactic acid yielded a similar product with a higher hydroxyl number of 412. In the same study, ring-opening introduced ethylene glycol, resulting in a 50/50 mixture of primary and secondary alcohols and a higher OH number of 398. The rigid foams made of lactic acid and ethylene glycol polyols demonstrated thermal stability to petroleum-based rigid foams for insulation. Algae polyol was recently produced using hydrothermal liquefaction, glycerol, and an acid catalyst. Unfortunately, the polyol had a high hydroxyl number of 590 and did not produce good foam. The Burkart group at UC San Diego recently devised a method to purify palmitoleic acid from residual oils collected during the manufacture of 3-omega fatty acids. Purified palmitoleic acid was oxidatively cleaved by ozonolysis to create azelaic acid, which was then polycondensed with diols to form microalgae-based polyols [37].

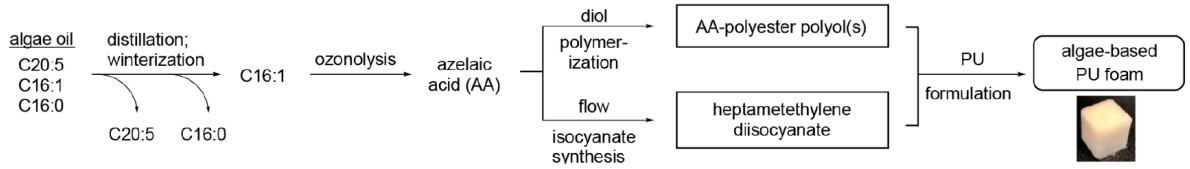

Figure 2.10: Azelaic acid and AA-polyester polyol from algae oil [37]

Figure 2.10, shows the schematic route that is utilized by Thien An Phung Hai et al. to produce PU foam. As mentioned earlier, the two main precursors to produce PU are Isocyanates and Polyols. From the previous section, it is understood that the algae oil is first used to produce azelaic acid, and later, this azelaic acid is 1. polycondensed with diols to form microalgae-based polyols, 2. azelaic acid using Curtius rearrangement in continuous flow chemistry is used to produced methylene diisocyanate. Finally, the polyester polyols are polymerized with methylene diisocyanate to produce the final PU foam [35].

2.4. Life-cycle Assessment

Life-cycle Assessment (LCA) helps in measuring and analyzing the environmental impacts of a service, product or process through assessment of its life cycle by a defined set of protocols starting from extraction, production, process development, consumption, and disposal. LCA will examine a process or product by understanding its impacts on the environment and hence helps the industrial sector to remodel their process or technologies to reduce the corresponding environmental impacts. When compared to Environmental impact assessment (EIA), which only focuses on the outcomes of the proposed development actions, LCA focuses on extending standard assessment boundaries and providing a broader scope to environmental assessment. The structure of the LCA was outlined by the International Standards Organization (ISO) with respect to the ISO standard 14040 comprising of four well defined methodologies, i.e., (1) goal and scope definition, (2) inventory analysis, (3) impact assessment, and (4) interpretation Figure 2.11 [9].

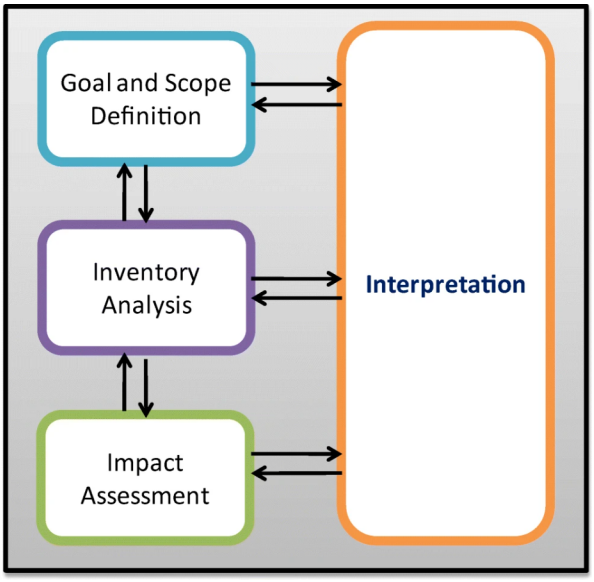

Figure 2.11: LCA methodologies

1. **Goal and Scope definition**: Defines the scope of the analysis, including the goals and system boundaries. The functional unit for the LCA is defined within this step. The functional unit describes a reference for what is being studied and how much or over what time frame (i.e. 1 kg plastic resin).
2. **Inventory Analysis**: documents material and energy flows that occur within the system boundaries, often referred to as Life Cycle Impact Assessment (LCIA)
3. **Impact Analysis**: characterizes and assesses the environmental effects using the data obtained from the inventory, often LCIA. LCIA expresses the LCIA data in common terms, usually concerning an equivalency factor, such as CO_2-equivalents for greenhouse gas emissions. Common LCIA categories include global warming potential, nonrenewable resource depletion, eutrophication, ecotoxicity, acidification, ozone depletion, smog formation, and human health (e.g. carcinogens, respiratory impacts, and non-carcinogens).
4. **Interpretation**: reviews the results of the LCA, identifies opportunities to reduce the environmental burden throughout the product's life, and provides conclusions and recommendations [18].

The LCA method is very flexible and specific to the field of analysis. Therefore, the application of LCA results according to the LCA methodology will be custom-designed and implemented. To achieve an authentic LCA, a stage-wise integration needs critical factors to be considered and clearly outlined.

2.4.1. Overview of LCA for bio-based fibres and resins (aviation sector)

The following section gives an overview of LCA performed on flax fibre and bio-based epoxy resin; selected materials are considered to be ecologically improved when compared to the currently used state-of-the-art materials in aviation.

Flax fibres

LCA comparing glass fibre with flax has showcased that flax fibre has relevant environmental benefits. Barth et al. determined the carbon footprint of flax fibre production to be 798 kg CO_2eq/t, with the highest impact coming from fertiliser production, followed by operation in the field. The third highest release of Greenhouse gases (GHG) is produced during the processing of the fibres. However, it represents a considerably lower impact than glass fibre production, which impacts 2.2 t CO_2eq per ton (Ecoinvent 3). Le Duigou et al. [24] studied the effect of flax fibre in thermoplastic composites. Showcasing that 30% w/w flax fibre Polypropylene (PP) composite is 5.6% lighter than GF/PP composite with similar fibre weight volume. Also, flax fibres have a lesser impact on the environment than glass fibres during production. Hence flax/ PP composites have an environmental impact of 20% lower than glass/PP. As the flax/PP composite parts are lighter than the glass/PP, this can lead to lower fuel

consumption and emission during flight, two key factors that the aviation industry is always aiming to achieve. Flax composite has a further advantage during End of life (EOF) if the composites are to be incinerated as flax fibre has a higher calorific value than glass fibres. Flax fibre with PP resin decreases the environmental impact by 10% for abiotic depletion and global warming and up to 20% for acidification. However, if a higher grade of flax fibre is used to achieve better strength and stiffness properties, the environmental advantage of flax may be little [3].

Another study by Duflou et al. comparing glass and flax fibre showed that flax fibres, due to their low mechanical strength, were not ideal materials for primary structural components compared to glass fibres. Also, flax fibres have relatively low bending and tensile properties, meaning that if they are used in applications with high strength equivalence, the environmental impacts are higher. Additionally, for impact class related to agriculture, like freshwater and land use ecotoxicity, the environmental impact of flax fibre composites are higher than the compared glass fibre composite [10].

Bio-based epoxy resins

Epoxy resins have been used in primary and secondary structures of aircraft for a long time. These resins are synthesized from materials originating from a petrochemical source. The aim is to investigate materials with natural renewable sources like cardanol, lignin derivatives, tannins, starches, and natural plant and tree oils, which can replace petrochemical materials. These natural materials can be utilized to produce low-cost epoxy resin, which is also environmentally friendly, as these can be epoxidized easily. A comparison between bio epoxy resin with natural fibre and glass-fibre/epoxy stated that the bio-based epoxy resin had reduced impact in most categories as listed in Table 2.1 when compared to petroleum-based epoxy. Also, the bio-based epoxy used for this study was prepared to utilize the biomaterials from waste and co-products of industrial processes (e.g. bio-fuel and wood pulp). The bio epoxy originating from co-products has an added benefit; it significantly reduces carbon footprint [3].

Table 2.1: Comparative impacts by one tonne of petroleum-based and bio-based epoxy composites [23]

Impact category	Units	Petroleum based-epoxy resin	Bio-Based Epoxy
Abiotic Depletion (ADP)	kg Sb eq.	59.4	0.01
Acidification Potential (AP)	kg SO2 eq	40.3	25.44
Eutrofication Potential (EP)	kg PO4-eq	6.6	6.9
Global Warming Potential (GWP)	kg CO2 eq	6663	4079
Ozone Layer Depletion Potential (ODP)	kg CFC11 eq	1.26E-6	0.00
Human Toxicity Potential (HTP)	kg 1.4 DB eq	490.44	545.17
Freshwater Aquatic Ecotoxicity Pot. (FAETP)	kg 1.4 DB eq	246.5	66.39
Terrestrial Ecotoxicity Potential (TETP)	kg 1.4 DB eq	29.1	228.63
Cumulative Energy Demand (CED)	MJ eq	2.16	1.90

Bio-Based Polyurethane

In their work, AndaFridrihsone et al. model a cradle-to-gate LCA for a pilot scale bio-based polyol production. Life Cycle Inventories are based on current regionalized rapeseed inventory, and experimental data for polyol synthesis is obtained directly from a pilot scale (50 L) reactor. The environmental footprint and key environmental hotspots for rapeseed oil-based polyols were identified using the Cumulative Energy Demand and ReCiPe methods, at both the endpoint and midpoint levels, with a focus on Global Warming Potential [12].

Overall, the total environmental impacts of both rapeseed oil-based polyol systems are similar, with the difference being several percentage points due to the different proportions of rapeseed oil and alkanolamine in the polyol. According to LCA results, the environmental impacts of bio-polyol production are primarily caused by rapeseed oil and alkanolamine production, followed by electricity; other synthesis inputs have a minor impact. The allocation method used in the rapeseed oil mill stage, whether by mass, economic value, or system expansion, has a significant impact on the results: the impact of bio-based polyols based on system expansion is significantly lower than that based on economic allocation [12].

This study found that using rapeseed oil as a bio-based feedstock for polyol production has a

significant impact reduction in terms of non-renewable energy use, lower GHG emissions, and water consumption when compared to petrochemical polyols. However, LCA results revealed that rapeseed oil-based bio-polyols performed worse in important midpoint categories such as land use, marine eutrophication, and ecotoxicity. Sensitivity analysis for rapeseed oil-based polyols was carried out by investigating electricity sources from various countries. The improvement or decrease in environmental aspects varies by less than 15% depending on the chosen electricity mix. Extensive research on rapeseed oil-based bio-polyols has yielded complex answers that are not unidirectional [12].

LCA on bio-composite materials have many challenges and gaps in study. Goal and scope definition is the most critical phase of the LCA. Various processes can affect the change in the life cycle of an application, including wastes & emissions and mass & energy flow. A comparison needs to be done on a functionally equivalent basis for composites, as they are typically lighter than their traditional counterparts. Furthermore, comparisons based on mass and constant volume do not yield accurate LCA results due to the varying mechanical properties of composites. Additionally, the lack of knowledge of in-service behaviour of bio-based materials causes service life to be rarely accounted. Also, studies that consider initial material properties do not consider material degradation during service or region-specific influences. Therefore, there is a gap in the knowledge concerning deterioration properties for composite materials .

2.5. Conclusion

For various reasons, natural fibre polymer composites have recently regained popularity. The desire for improved fuel efficiency in automobiles, cheaper and better building materials, and a growing public concern for environmental preservation are just a few examples. Natural fibre reinforced composites (NFRCs) have piqued interest in recent years due to their ease of manufacture, the subsequent increase in productivity, cost reduction, decreased density and weight, and utilization of renewable resources. However, there are numerous issues with the fabrication of bio-based composite materials, including natural material compatibility with synthetic polymers, dimensional stability, and processability issues. In addition, it is vital to produce a suitable interface (or interphase) in any good composite so that applied stress can be passed between the two different materials. Also, most of the NFC being used currently in the industries employ petroleum-based resins (ex. epoxy). The need of the hour is also to minimize the use of petroleum-based epoxies and try to replace them with bio-resins. However, before commercially viable NFRCs can be widely used in engineering applications, more research is needed to address severe material and production challenges. This research aims to manufacture a fully bio-based material and study its properties whilst showcasing what could be the future application for this material.

3

Research Definition

The thesis will focus on manufacturing a Thermoplastic composite, which comprises a bio-based resin, and finally, understand the impact this product will have on the environment. The objectives resulting from this are discussed insection 3.1, following which the main research question is derived in section 3.2 and finally, the hypothesis for this work in section 3.3.

3.1. Research Objectives

This research aims to manufacture and characterise a thermoplastic natural fibre composite using a bio-based polyurethane resin. After manufacturing the natural fibre composite, an analytical Life cycle assessment of the product will be performed to understand the impact of CO_2 of the system.

To achieve this objective, it is first necessary to understand the characteristics of the thermoplastic resin—the effect on the quality of the natural fibre composite when a different manufacturing method is used—following by testing it using various ASTM standard methods. Finally, conclude by performing a rudimentary LCA of the sample.

3.2. Research Questions

Based on the objectives of the research. The research question can now be narrowed down to the following:

"What are the characteristics and life-cycle impact of a manufactured thermoplastic natural fibre composite when using a novel algae-derived polyurethane resin?"

The main question can be broken down into four aspects, each aspect characterized as a sub-question.

1. What are the best manufacturing methods to utilize the available Polyurethane resins?
2. What are the thermal characteristics of the resin?
3. What is the morphology of the composite cross-section, and how is the interface between the resin and the natural fibre?
4. How does the addition of the resin help the fibre concerning moisture absorption?
5. How does the utilized Polyurethane compare to commercial polyurethane in terms of environmental impacts?
6. How much CO_2 is embodied in the manufactured Flax/PU composite?

3.3. Hypothesis

The main hypothesis is that the manufactured natural fibre composite, while displaying comparable properties to other commercial setups, also has a comparably lower impact on the environment.

4

Materials and Methodology

4.1. Flax Fibres

Bcomp Ltd. (Fribourg, Switzerland) provided the wet spun UD-woven flax fibre fabrics (ampliTexTM UD type 5025) with an area weight of 275 g/m^2. Flax fibres decompose at a relatively low temperature of 170-190 °C, depending on the environment and length of exposure to high temperatures. As a result, the polymers utilized to create Natural fibre reinforced composites must permit processing below the temperature at which the fibre degrades.

4.2. Thermoplastic Resin

The resin chosen for this study is polyurethane. Polyurethane(PU) was supplied by the University of San Diego in the form of thermoplastic pellets(TPU) and solvent-based polyurethane (SBPU, comprising 60% of MEK solvent in the total mass). The reason for selecting these resins is due to their bio-based algae origin. The University of San Diego Burkart group has developed this 75% bio-based polyurethane utilizing algae to produce polyol, one of the main precursors to make PU. The thermoplastic pellets have a density of 1.14 g/ml, and solvent-based polyurethane has a density of 0.85 g/ml. A significant difference between the two polyurethanes is the percentage of hard and soft segment chains present in the polyurethane; the thermoplastic pellets comprise 80% hard segment chains, while the solvent-based PU consist of 71% soft segment chains.

4.3. Rheological measurements

Using the Thermo Scientific Haake MARS III Rheometer, the viscosity of the polymer was determined following ISO 11443. The test was conducted using the plate-plate method (8mm diameter plate) and using a temperature sweep program by heating the sample from 30° C to 160° C, a gap thickness of 1mm was maintained during this test. Samples of thickness 1mm were prepared in order to avoid slippage between the interface of the polymer and plate.

4.4. Thermogravimetric (TGA) measurements

The thermal stability and fraction of volatile components of the polymeric resin are determined with the Thermogravimetric (TGA) measurement. This is done by closely monitoring the weight change of the sample for a determined heating rate. Samples weighing between 5milligram and to 30milligrams were prepared by placing them inside the ceramic crucible. The samples were then placed in the PerkinElmer TGA 4000 machine and heated up to 500° C at a rate of 10° C per min. To obtain a good statics and repeatability of results 3 trails are performed for each sample.

4.5. Differential Scanning Calorimetry (DSC) measurements

To establish the temperatures at which the phase transition occurs, including glass transition temperature, melting temperature, and crystallization events, a differential scanning calorimetry (DSC) measurement is performed on the resin according to ISO 11357 standards. A specimen weighing between 5 and 25

milligrams is prepared for the measurements. A sample weighing ≈ 8mg is placed inside a DSC pan which is sealed by a lid using a hand press. The samples were then subjected to a heat-cool-heat cycle from a temperature of -50° C to 200° C at a rate of 5° C per min using the TA instruments DSC 250. The first heating cycle erases previous thermal history by heating the material above a transition. For different iterations of a sample the weight is kept uniform across the trails in order to achieve a high degree of repeatability.

4.6. Thermoplastic Polyurethane Film production

Thermoplastic film width of 90mm and approximately 150μm were produced using the Joos 500KN press. The Polyurethane provided by the University of San Diego is in the form of pellets, which are pressed up-to the melting temperature and the cooled down to room temperature to produce the films.Section 6.1 goes into the details about the preparation of the films and the various Temperature-pressure cycles used to achieve films with zero voids.

4.7. Composite Manufacturing

Pre-dried flax fabric (vacuum oven at 110°C for 15 minutes) and pre-dried polymer films were used to create the natural fibre thermoplastic composites by stacking them alternately in a steel mould. The number of alternating layers needed for flax fabric and polymer film was calculated using a reference fibre volume content of 50%. Composites with a nominal thickness of 2 mm were created by stacking six unidirectional (UD) flax layers and 7 layers of PU film. Chapter 6 discusses the manufacturing of the natural fibre composite.

4.8. Contact angle measurement

Using the KSV CAM200 goniometer, the contact angle measurement was performed. The Sessile drop method measured the advancing and receding contact angles between distilled water on polymer film and technical flax fibres at room temperature (20° C) and 50% relative humidity. The sessile drop method involves placing a droplet on a solid sample, usually water, and using a high-resolution camera to capture an image of the drop. The software then automatically calculates the contact angle. A surface is referred to as hydrophilic if the water contact angle is less than 90° and hydrophobic if the contact angle is greater than 90°. In many applications, hydrophilicity and hydrophobicity are crucial because it provides a rapid and non-destructive approach to assessing surface chemistry.

4.9. Water Absorption test

The natural fibre composite's water absorption is tested using the ASTM D570 standard. The experiment evaluates the water absorption rate by immersing the specimen in water for a long time. To characterize this feature, this test technique examines the percentage increase in weight of the sample following the experiment. This property must be evaluated since polymers or fibres tend to absorb water, which may cause the plastic's properties to change as characteristics like electrical insulating resistance and mechanical strength are closely related to the moisture level of that type of material. Therefore, when doing this test, the following criteria must be considered: the time of immersion, the temperature of the water, the thickness of the sample, and the type of material. For this experiment, a sample size of 30mmx30mm is cut and placed inside distilled water for 24hrs. The measurement and appearance of the samples were checked before and after the test.

4.10. Tensile Testing

4.10.1. Tensile Test of Resin

Tensile testing were performed on polymer dog bone specimens at 20°C and 50% RH using as Zwick 20KN Universal testing machine fitted with a 1KN load cell. The tests were carried out at a displacement-controlled rate of 50 mm/min with the help of a universal testing equipment fitted with a 100 N capacity load cell. First, the sample was prepared by taking 10 grams of TPU pellets and placing them inside a Teflon mould as shown in Figure 4.1. Next, this Teflon mould is placed inside an oven and heated to the melting temperature of the resin. After cooling down, a bar of TPU is obtained and is shwon in Figure 4.2, and as seen from this image, a large number of air bubbles are present on one surface

of the neat resin bar. A grinding machine removes these bubbles, and a final polishing is done to this surface. These bars are then placed under a dog bone die, and a dog bone shape is cut out as shown in Figure 4.3. These dog bone specimens are then placed between Mechanical clamps as represented in Figure 4.4. Following this, the tensile test is performed.

Figure 4.1: TPU pellets placed inside Teflon mould

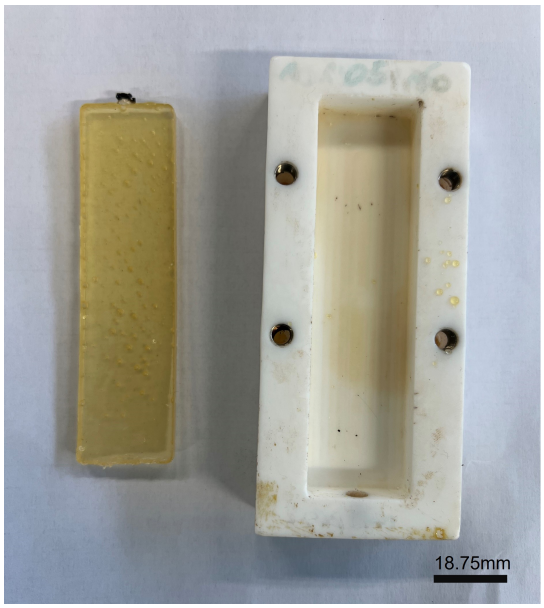

Figure 4.2: TPU pellets after melting and cooling into a block

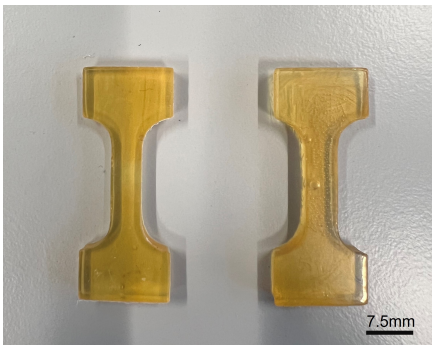

Figure 4.3: TPU dog bone sample ready to be tested

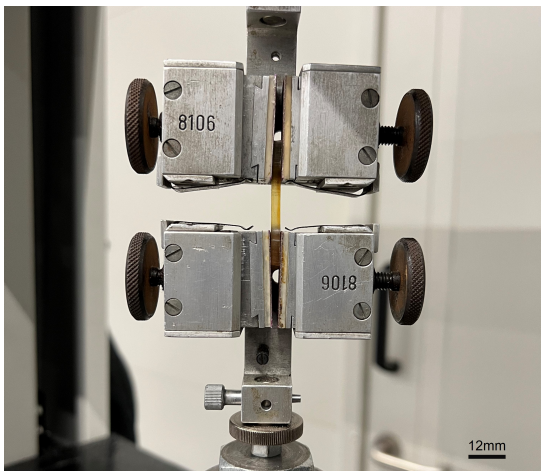

Figure 4.4: Mechanical clamps used for the tensile test

4.10.2. Tensile Test of Composite

The Zwick 10KN universal testing machine was utilized to test the tensile property of the manufactured composite materials. A specimen dimension of 150mm in length and 15mm in width with a thickness

of approximately 2mm is cut and used for this experiment. The tests were carried out at a displacement-controlled rate of 5 mm/min.

4.11. Flexural testing

The flexural characteristics of the composite were measured using ISO 14125 three-point bending measurements. NF composites with longitudinal and transverse fibre orientations were tested. A length of 40 mm was chosen between the two supports to enable a span-to-thickness ratio greater than 16. Flexural tests were carried out on a Zwick 20KN universal testing machine fitted with a 1 kN load cell at a displacement-controlled rate of 4 mm/min.

4.12. Dynamic mechanical analysis(DMA) measurement

DMA, or dynamic mechanical analysis, was utilized for quality assurance. The term "DMA" describes how plastic materials react to dynamic or cyclic pressures. These responses could be described as a function of temperature, frequency, or time in terms of the storage modulus (elastic modulus, G'), loss modulus (viscous modulus, G"), and tan (damping coefficient, G"/G'). The storage modulus, which is frequently correlated with stiffness, is a gauge of a sample's elastic behaviour. The dissipation of energy for a material under cyclic loading, also known as damping, is called loss modulus. The results are commonly presented as a graphical plot of G', G", and tan vs temperature, indicative of molecular structure, materials behaviour, product, and processing attributes. Samples with a width of 5mm and length of 30mm are used for the experiment using the RSA-G2 Solids Analyzer by TA instruments. A Standard Oscillatory Temperature Sweep was performed on the samples from a temperature of -100 ° C to 80° C at rate of 2° C per minute.

4.13. Microscopy

To understand the interface between the flax and the thermoplastic resin, microscopy was performed. First, the samples for microscopy were prepared using a mould into which the samples were placed, and the EpoFix resin (Figure 4.5) was poured at a ratio of 25:3 resin: hardener. After the resin cures, the surface of the sample is improved with a grinding machine by changing the grit papers grain size from 200μm to 5μm. Following this, polishing was performed on the surface to achieve a good surface for testing, as shown in Figure 4.6. The samples were then placed under the Keyance Laser microscope to check the interface properties.

Figure 4.5: EpoFix resin and hardener

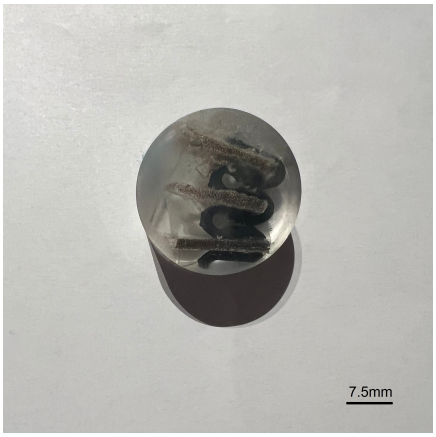

Figure 4.6: Sample prepared for microscopy after grinding and polishing

4.14. Life Cycle Assessment (LCA)

A life cycle assessment of the product is performed after the manufacturing stage. Life cycle assessment is a cradle-to-grave or cradle-to-cradle analytic technique used to examine the environmental implications associated with all stages of a product's life, beginning with raw material extraction and continuing through materials processing, manufacturing, distribution, and usage. For this thesis, utilizing the cradle-to-gate approach, a conceptual LCA is performed, which is the first level of LCA based on limited environmental elements of a few life cycle stages. The objective of the LCA will be to determine the embodied carbon dioxide in the system. The findings are beneficial for qualitative reporting of assessment results and giving an idea of how the natural fibre composite can further be developed in a sustainable manner.

5

Polyurethane Investigation

Studying the natural composite's properties is one of this thesis's primary research questions. However, more information about the resin must be gathered before doing so. Mainly, the thermal properties of the resin indicating what region the materials T_g, T_m and the degradation temperature lie in. Therefore, the experimentation phase starts by conducting Rheology measurements, Thermogravimetric (TGA) measurements and Differential Scanning Calorimetry (DSC) measurements to gather this information. Section 5.1, section 5.2 and section 5.3 showcase the results obtained for rheology, TGA and DSC, respectively. Finally, every section also discusses how the achieved data will be utilized while manufacturing the natural fibre composite.

5.1. Rheology measurements

The melt viscosity of the polymer material was determined using rheology measurement using the plate-plate method, with a temperature sweep program from a temperature of 50° C to 150° C. Samples of diameter 8mm and thickness 1mm are prepared using a small circular die. Then a sample was placed on the bottom plate, and the top plate was moved to the top of the resin sample to apply a small load on the resin sample. This ensures that the sample is firmly paced between the two plates and that there is no slippage. First, Thermoplastic polyurethane pellets (TPU) were tested, and the viscosity vs temperature plot for this can be seen in Figure 5.1. From the plot, it is evident that the pellets start to melt around a temperature of 110° C, and the viscosity keeps decreasing with increasing temperature. This temperature is crucial as the pellets need to be prepared into films for manufacturing the composite. Hence, to allow the pellets to flow easily and form a uniform, void-free film, the temperature of 130° C is chosen for all of the experiments ahead. This temperature is also chosen for composite manufacturing due to the lower viscosity of the resin. At this temperature, the resin can flow through the fibre and create a good bond between the fibres and resin, resulting in a stiff composite. On the other hand, Figure 5.2 illustrates the viscosity vs temperature plot for the SBPU resin. Here it can be noticed that the viscosity keeps steadily declining from 40° C onwards, and beyond 100° C, the viscosity is extremely low. This is primarily due to the high percentage of soft segment chains in the PU structure. Also, as a high percentage of solvent is present in the material, it tends to flow more easily than the TPU pellets. Due to the constantly decreasing viscosity value, choosing an exact processing temperature is not easy. However, from the literature, it is known that MEK(Butanone) evaporates at a temperature of 80° C, and the MEK solvent needs to be removed entirely from the system. Hence, 80° C is chosen as the processing temperature for the SBPU resin.

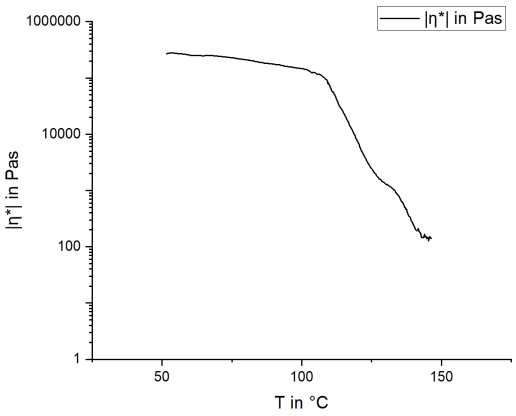

Figure 5.1: Viscosity vs temperature for TPU resin

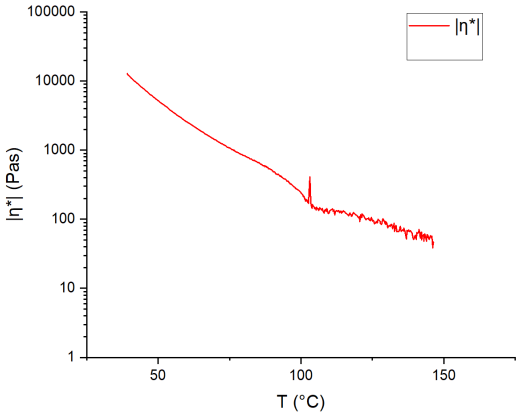

Figure 5.2: Viscosity vs temperature for SBPU resin

5.2. Thermogravimetric analysis (TGA)

The experiment began by cutting a sample of mass between 5mg to 30mg. shows the sample weight for Thermoplastic Polyurethane pellets (TPU), solvent based polyurethane (SBPU) and flax fibre. The cut sample was then placed inside the ceramic crucible, which was then placed on the tray of the TGA 4000 (PerkinElmer) as shown in Figure 5.3. The machine then picks the crucible and places it inside the oven where it then performs the program that has been selected. There are two programs that were used and they are as follow:

Program 1: Ramp Up

For the ramp-up, a program starts once the crucible shifts from the tray into the oven. The oven starts to heat up at a rate of 5° C per min from 30° C up to 500° C. This program gives an understanding of at what temperature the resin disintegrates. If there is a significant drop in weight, this indicates that volatiles is present in the material. Figure 5.4 is the weight change (%) vs temperature for the thermoplastic polyurethane pellets. The graphs show that the change in weight for the TPU is meager, specifying that the resin is stable and it beings to lose weight at a temperature close to 270° C. Similarly, Figure 5.5 that flax fibre is also thermally stable and being to lose weight at a temperature of 230° C. However, the SBPU does not behave the same as the TPU, and it can be seen in Figure 5.6 that there is a huge loss in weight upto 128° C. This huge weight loss is suspected to be because of the Butanone (MEK). As butanone has a boiling point of 80° C, this solvent would have evaporated out of the resin, causing the weight to drop drastically. For the next trial with SBPU, the SBPU was first dried in an oven at 70° C for 24 hours and let to cool down. The dried sample was then placed in the crucible and tested for a ramp-up from 30° C to 500° C. This proved a successful attempt, as seen in Figure 5.7, where the weight change remains constant till 235° C, beyond which the material starts to lose weight.

This test concludes that the TPU pellets and flax fibre are stable without any pre-treatment, and a pre-treatment may be required for the SBPU before manufacturing the natural fibre composite.

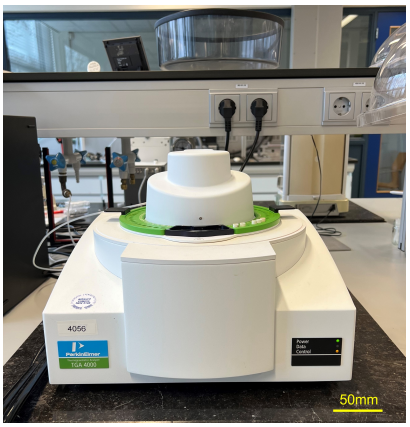

Figure 5.3: Perkin Elmer TGA machine

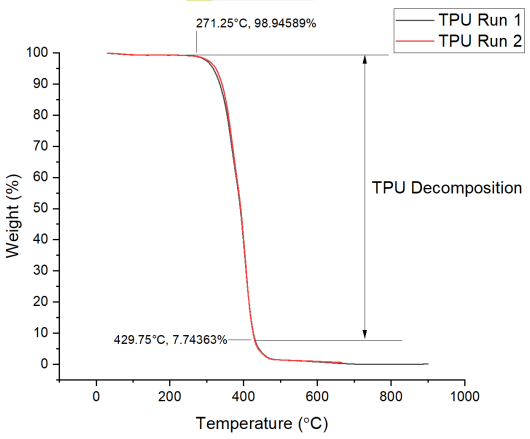

Figure 5.4: TGA thermogram of Thermoplastic polyurethane pellets

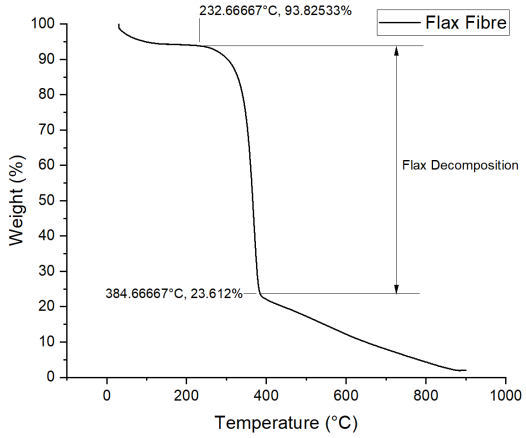

Figure 5.5: TGA thermogram of Flax Fibre

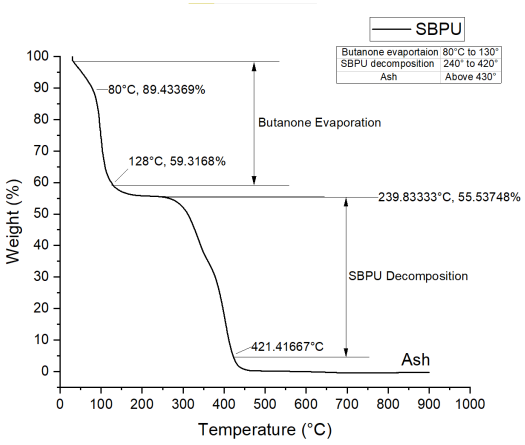

Figure 5.6: TGA thermogram of SBPU

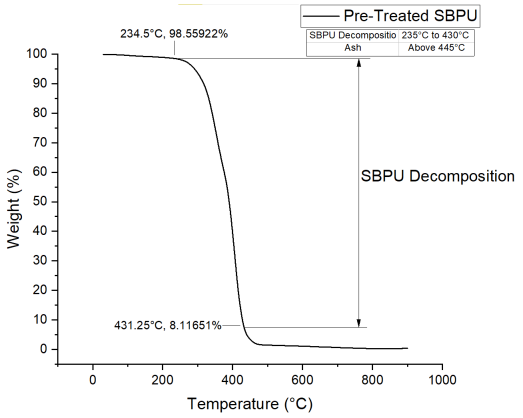

Figure 5.7: TGA thermogram of SBPU after drying in the oven at 70° C

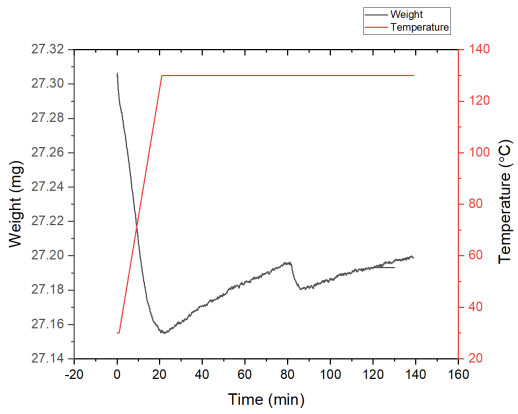

Figure 5.8: Isothemal hold of Thermoplastic polyurethane pellets at 130° C for two hours

Program 2: Isothermal Hold:

As mentioned earlier, the TPU pellets need to be melted to create films of 150μm thick films. Since these films are made in the press, they are subjected to the melting temperature for a moderate amount of time, and an isothermal hold of the sample at the melting point is performed to observe if there is any

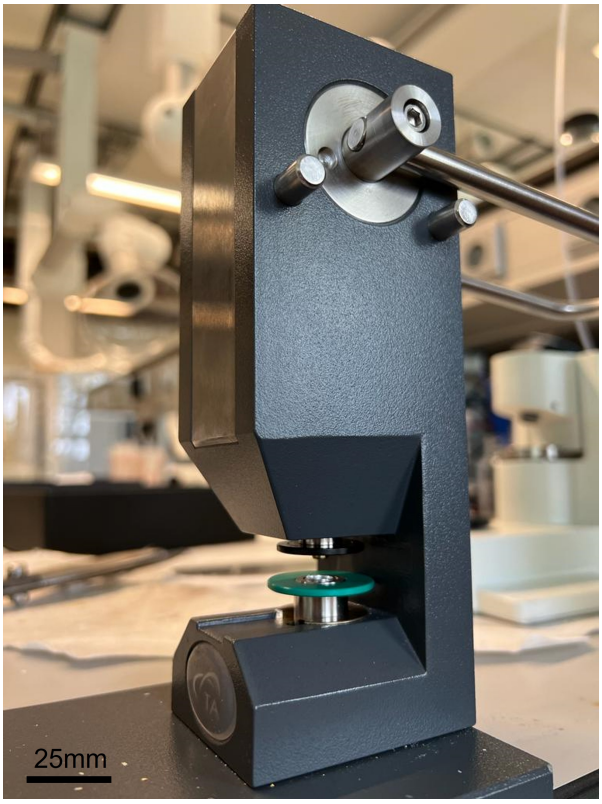

Figure 5.9: Press used to cold weld the pan and lid for DSC

change in weight with respect to time. Therefore, the TPU pellets were placed in an isothermal hold at a temperature of 130° C (this temperature was chosen after performing the rheology measurements) for 2 hours. Figure 5.8 displays that the TPU pellets have no change in mass for this duration, implying that the creation of films in the press will not affect the material.

5.3. Differential Scanning Calorimetry (DSC) measurements

After identifying the thermal stability of the resin, differential scanning calorimetry (DSC) measurements of the resin were performed. The DSC results showcase the glass transition and melting temperature of the resins. The experiment starts with the preparation of the sample and then placing them into the TA DSC 250 machine and which the obtained graphs are studied to give an understanding of the various temperature regions.

The samples must be prepared using a TA standard pan and lid. First, each sample was weighed on a weighing scale. The sample was then placed inside the pan, and before placing the lid on top of the pan, a small hole was pierced through the lid. This is so that any gasses during the heating cycle can escape from inside the pan. Next, the pan and lid must be sealed together, and this was done using a manual press as shown in Figure 5.9. This manual press cold weld the pan and lid together, ensuring that the sample is secure inside. Parallelly, a reference pan without any material inside was created because the DSC machine compares the heat flow of the reference pan with the sample pan. Finally, the reference and sample pans are placed in the tray of the DSC machine, and the required program is started. The program used for both the TPU and SBPU resin is the heat-cool-heat program. The first heating cycle ensures that any thermal history of the material is erased, and the data used for the study is gathered from the second heating cycle.

First, the DSC is performed for the TPU pellets, the weight of different samples were kept almost similar, close to $8mg$, this is to achieve good repeatability between trails. Three trials were performed for this experiment to achieve repeatability of results. The sample inside the oven is subjected to a heat cool heat cycle which was as follows: 1^{st} heating cycle -50° C to 200° C at a rate of 5° C per min, cooling cycle: 200° C to -50° C at a rate of 10° C per min and 2^{nd} heating cycle: -50° to 200° C at a rate of 5° C per

min. The TPU pellets' DSC graph is illustrated in Figure 5.10. Much data can be collected from this graph. As it is known from the literature that Polyurethane comprises a hard and soft segment, it is expected that the material comprises two glass transition temperatures, one for the hard segment & one for the soft segment and a melting temperature. This is proven correct as three peaks are observed in the graph Figure 5.10. The first peak is noticed when there is a change in heat flow at the temperature -47° C to -36° C, which indicates that the glass transition temperature of the soft segment lies in this region ($T_g ss$). The next noticeable change of heat flow is at the temperature between 10° C and 36° C, and this is the glass transition region for the hard segment of the polyurethane pellets ($T_g hs$). The maximum heat flow for this region is at 24° C. Therefore, it is labelled as the glass transition temperature for the hard segment. The final change in heat flow is noted at the temperature of 125° C to 145° C, beyond which the heat flow constants keep declining as the material starts to lose weight heading towards ash, as seen in the TGA graphs in the previous section. The region between 125° C to 145° C is described as the melting region where the pellets slowly change from a solid to a liquid state. From this range, an educated guess is made, and 130° C is considered the melting temperature (T_m) for further experiments.

Next, the DSC for the SBPU was performed. Similar to the TPU, the sample weight for the different tests were maintained at the same amount. The SBPU was first pretreated in the oven at 70° C to remove the MEK solvent inside the resin, and then the sample was prepared. After placing the samples in the DSC machine, the program was started. The heat-cool heat cycle for the SBPU was similar to that of the TPU. With a 1^{st} heating cycle of 25° C to 200° C at a rate of 5° C per min, cooling cycle of 200° C to -50° C at a rate of 10° C per min and 2^{nd} heating cycle of -50° to 200° C at a rate of 5° C per min. The SBPU behaves differently from the TPU, as seen in the representation Figure 5.11. The only peak and change in heat flow is observed at a temperature range between -46° C and -22° C, indicating that the glass transition temperature lies around this range. After studying the literature, it is known that the T_g in this region is that of the soft segment of Polyurethane. Beyond this temperature, there is no change in heat flow in the materials. This is because the hard segment present in this resin is very low, about 20%. Hence, no significant peak can be seen for the glass transition of the hard segment of the PU.

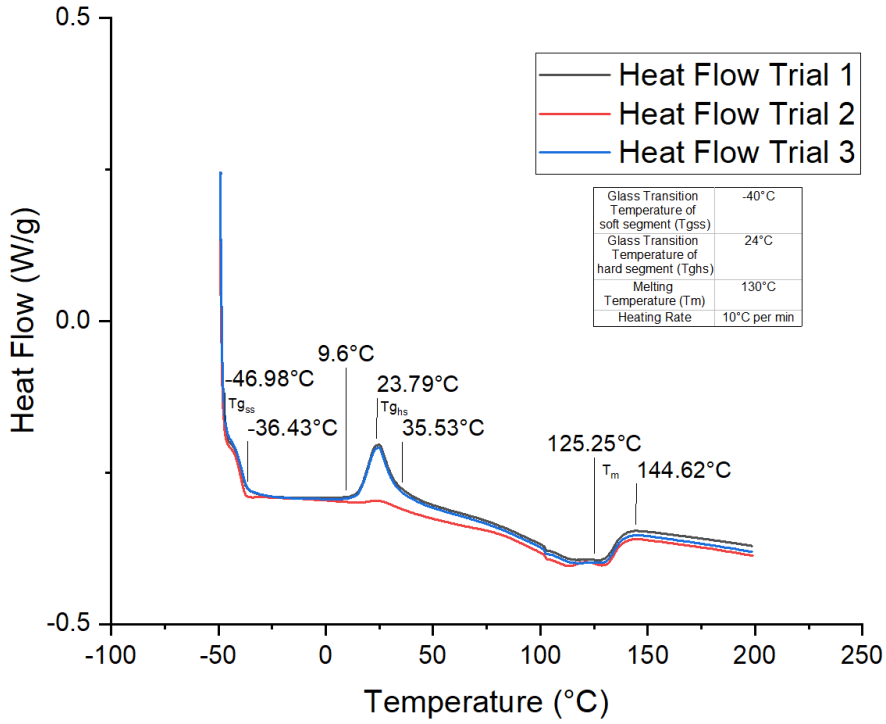

Figure 5.10: Differential Scanning Calorimetry (DSC) curves for Thermoplastic polyurethane pellets

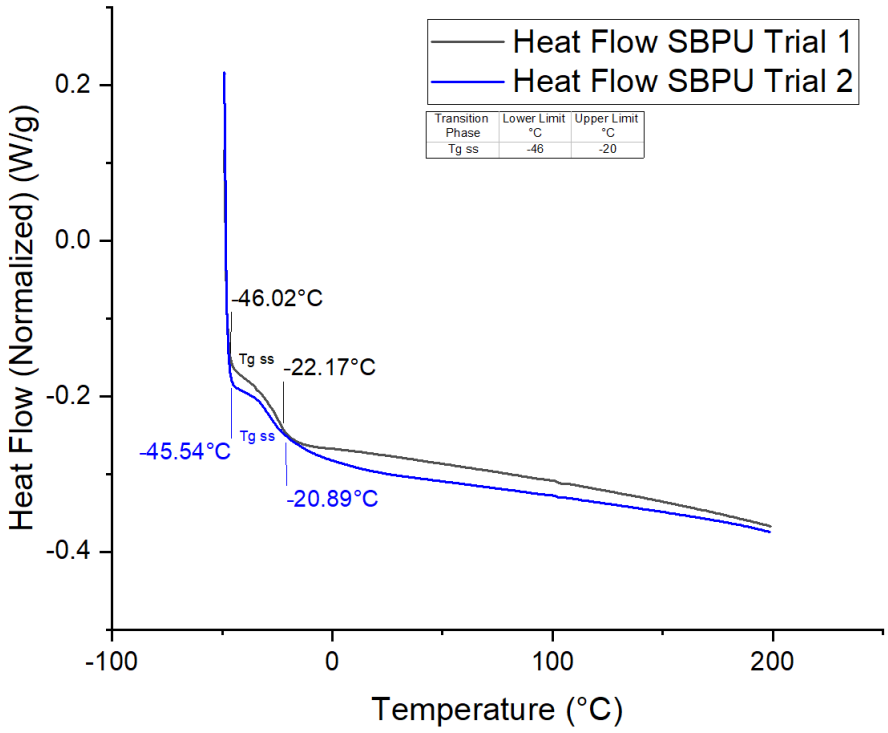

Figure 5.11: Differential Scanning Calorimetry (DSC) curves for SBPU

5.4. Discussion

Performing the rheology, Thermogravimetric analysis and DSC was crucial as this helped to characterize the TPU and SBPU resin. The critical finding from rheology was the viscosity and temperature when the TPU pellets start to melt. As these TPU pellets need to be made into films, a temperature must be fixed to achieve a uniform and void-free films. Therefore, 130° C was chosen as the processing temperature to produce the films. From TGA, it was evident that the TPU pellets are stable up to 270° C. Also, at 130° C, the pellets had no weight loss for 2 hours, which could be crucial during the production of the films. Finally, with the DSC measurements, the transition temperature was identified for the TPU pellets. The first glass transition temperature of the soft segment is at -40° C, and the glass transition of the hard segments is at 24° C. Also, melting temperature is noticed at a temperature of 130° C, which backs the findings of the rheology measurement where the pellets showcase a change in viscosity around 120° C.

On the other hand, the rheology result of the SBPU showcased that the viscosity of the resin constantly keeps decreasing from 40° C. This could be due to the high MEK present inside the solvent. Due to this MEK, the TGA plot shows a 40% loss in weight of the resin, indicating that the MEK evaporates from the system between 40° C and to 100° C. Finally, the DSC showcases only one peak owing to the soft segment of the material, which is at a temperature of -40° C. This is because only 20% hard segment is present in the system. Therefore, for the creation of the composite more preference is placed on the TPU pellets as it is more stable than the SBPU. However, an attempt is made to create a Flax/SBPU panel. The following chapters will go into more detail about composite manufacturing.

6

Composite Manufacturing

This chapter comprises the manufacturing methods used for producing natural fibre composite using polyurethane resin. The film stacking manufacturing method is the chosen technique for Thermoplastic Polyurethane(TPU); the inspiration is taken from the work of Woigk et al. [41] to utilize this manufacturing process. The data observed in the work of Woigk et al. [41] is of interest as they also used thermoplastic bio-based resins. Hence for the results, a comparison is made with the data from Woigks work. Section 6.1 details the production of a 150μm film, the challenges faced, and the final solution to produce repeatable films. After producing the films, the next step is to create the composite, section 6.2 explains the manufacturing of the composite for the TPU. For the solvent-based polyurethane(SBPU), the hand layup method is chosen due to the resin's flowability. Section 6.3 goes into more depth about the SBPU and the hand layup method. Finally, section 6.4 discusses the method used the prepare the samples for the testing phase.

6.1. Thermoplastic Film Preparation

The film for the Thermoplastic polyurethane pellets was created using a 500KN Joos Press. First, the pellets were weighed and portioned into smaller batches of 10g each. Next, one batch of the 10g pellet was placed inside a closed mould. The mould with the TPU pellets inside was then placed inside the press. From the data of DSC, it is known that the PU pellets start to melt around the temperature of 130° C. Therefore, the idea was to heat the mould with the pellets to the T_m, allowing the pellets to change their phase from solid to liquid and then cool it back to room temperature. Trial and error were performed with various temperature and pressure cycles to obtain the best films with the lowest or no voids. For the first film, after placing the mould inside the press, the press was heated to 130° C and immediately once the temperature was reached, a pressure of 10 bar was applied on the mould. With this pressure, the mould was allowed to stay at 130° C for 10mins, after which the press was put to cool to room temperature while maintaining the pressure. The mentioned cycle is represented in Figure 6.5. However, the film produced from this cycle had inferior quality as it had many voids inside it, as shown in Figure 6.1. For the next iteration, after ramping up the temperature to 130° C and applying 10 bar pressure, the mould was held at 130° C for 1 hour. From the TGA isothermal hold data, it was understood that there would be no change in weight for the pellets for up to 2 hours. After 1 hour at 130° C and 10 bar pressure on the mould, the press is cooled down with maintaining 10 bar of pressure. The film produced using this cycle also showcased a high amount of void in the film, similar to the previous film. Following this, for the third cycle, a dwell time was added after the ramp up to 130° C, and the pressure was applied at 130° C for only 5mins. After which, the mould was cooled down, maintaining the 10 bar pressure, as shown in Figure 6.7. The film produced using this cycle was of good quality, as shown in Figure 6.3; the voids were only towards the sides of the films, and as the films were to be cut out to 150mm length and 90mm width, the voids in the edges did not seem to be a problem. However, the films created using the above three cycles were of thickness about 250μm, and this was due to the mould being closed, which what a gap of 300m between the dies. Hence, the mould was replaced by two aluminium plates, and 150μm thick shims were added between these plates to provide the required thickness for the films. Using these plates, the cycle shown in Figure 6.8 was

used, which had a increased dwell time(15mins) before applying pressure onto the plates. Results in films with zero voids and thickness of 150μm thickness were produced, as shown in Figure 6.4. The reason for obtaining void-free films was because of the plates, which allowed air to escape the system, unlike the closed mould system that was used previously. Therefore, using cycle 4 (Figure 6.8) and the aluminium plates, 40 films of thickness 150μm were created.

Figure 6.1: Film 1 comprises of many voids

Figure 6.2: Film 2 has many voids in the center of the film

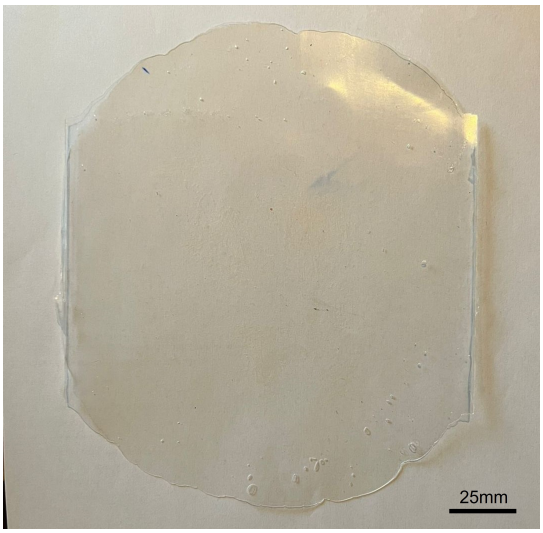

Figure 6.3: Film 3 has all the voids pushed to the sides

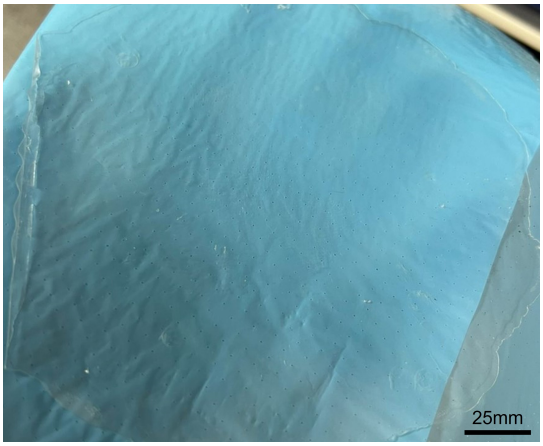

Figure 6.4: Film 4 is void free

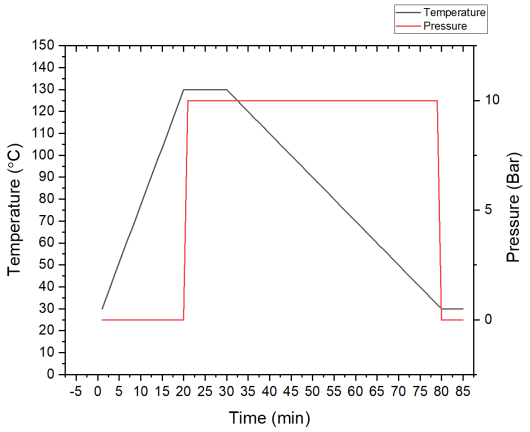

Figure 6.5: Temperature Pressure cycle for Film 1

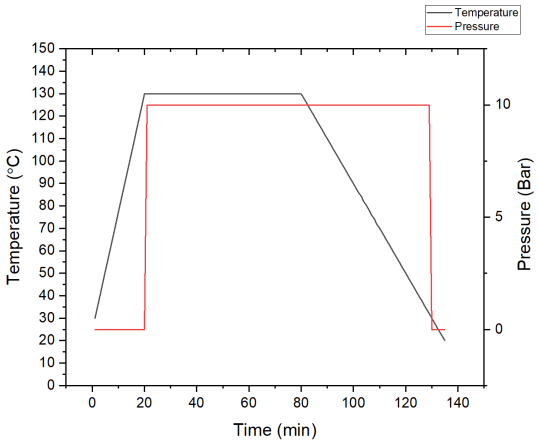

Figure 6.6: Temperature Pressure cycle for Film 2

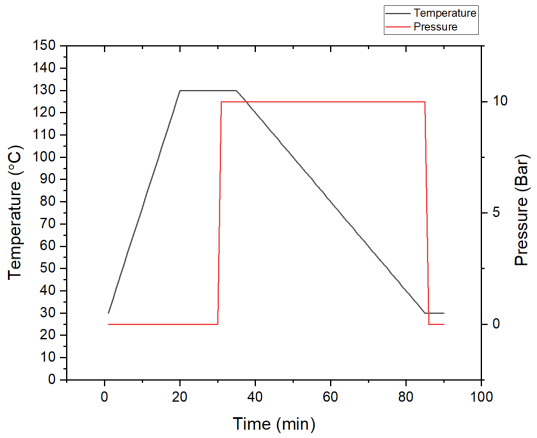

Figure 6.7: Temperature Pressure cycle for Film 3

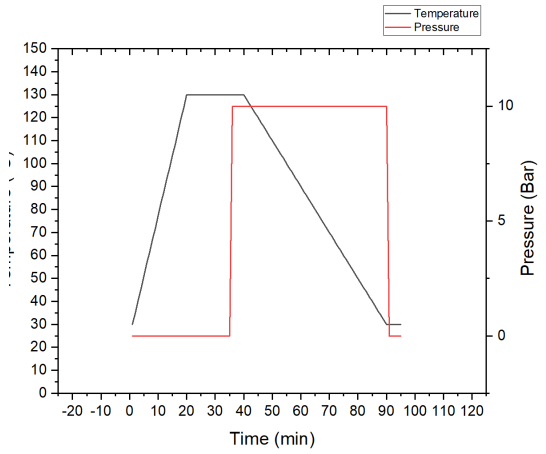

Figure 6.8: Temperature Pressure cycle for Film 4

6.2. Film stacking manufacturing

The thermoplastic polyurethane pellets that were reshaped into films were then ready to manufacture the composite. The next step is to cut out the flax fibre into rectangular shapes of dimensions 150mm x 90mm, and this was done using the Gerber cutting machine as shown in Figure 6.9. Each one of these flax fabrics of dimension weighs about 3.3g. The polyurethane films were prepared in a manner to achieve a 50% fibre volume fraction. After the flax fabrics were cut into the required dimension, they were stacked alternately with PU films in a steel mould. A schematic of this stacking is shown in Figure 6.10. Six layers of flax fibre and seven films of PU are used to create the natural fibre composite. Before the stacking, these six layers of flax were placed inside the oven at 110° C for 15 minutes to ensure that any moisture in the fibres was removed and helped in better adhesion of the resin and the fibres. After placing in the mould, the final stacked layers are as shown in Figure 6.11. Finally, an upper die is placed in the cavity of the mould. The closed mould was then placed in a 130° C pre-heated press (Joos 500KN press), and a piston pressure was applied, resulting in a cavity pressure of 1MPa. After 10 minutes, the press is cooled back to room temperature while maintaining the 1MPa pressure. Following the cooling down, the desired natural fibre composite is achieved and can be seen in Figure 6.12. This procedure is repeated four more times, creating five natural fibre composite plates. Four plates have fibres in the 90° orientation and the final in 0° orientation.

Figure 6.9: Gerber cutting machine cutting out flax fibres in transverse direction

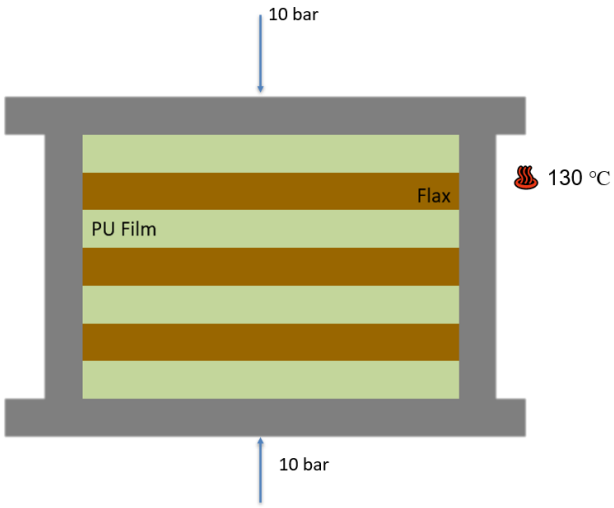

Figure 6.10: Schematic representation of the film stacking method

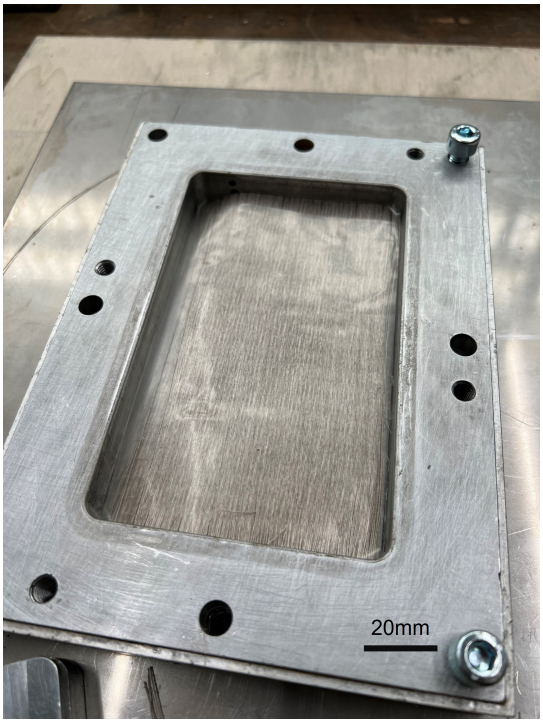

Figure 6.11: Natural fibre composite film stacked before placing under the press

Figure 6.12: Natural fibre composite film stacked after placing under the press

6.3. Hand Layup

On the other hand, the solvent-based polyurethane was manufactured using the hand lay-up method. As it comprises about 75% soft segment in the resin and a high percentage of Butanone(MEK) in the

system, this resin is in the liquid state. Similar to the Film stacking method, the manufacturing begins with cutting the flax fabric into the desired size, 150mm x 90mm. Next, these flax fabrics were dried in the oven at 110° C for 15mins for all the moisture in the fabric to be removed; this is to ensure that the resin flows well through the fibres as well. The experiment started by placing the first layer of flax fabric on the steel mould. Keeping 50% fibre volume fraction in mind, 10ml of resin was poured onto the fabric. This resin was then evenly spread across the surface of the flax fabric using a 3M resin spreader tool. After completely spreading the resin to every corner of the fabric, the fabric was allowed to rest at room temperature for 20 minutes before placing the next layer on top; this was done because of the MEK in the solution. The idea was to allow the MEK present in the layer to evaporate, allowing just the neat resin to be left in the system. After 20 minutes, the next layer of fabric is placed on top of the completed first layer, and similarly, the resin is poured onto the surface, spread evenly, and rested for 20mins. Likewise, a total of six layers of flax fibre are hand laid to create a composite of the nominal thickness of 2mm as shown in Figure 6.13. In the Figure 6.13, it can be seen that all of the fabric layers are placed over a film. This is to ensure that the composite can peel off easily after curing. The mould is closed with the upper die and placed in an 80° C pre-heated press(Joos 500KN) for 5 hours. After closing the press, a pressure of 2MPa was applied to the mould. Post 5hours, the mould was cooled back to room temperature while maintaining the pressure. The result of this cycle is seen in Figure 6.14, where most of the resin was squeezed out of the system. The cause of this was due to human error, as the pressure applied was probably higher than required. Therefore, for the next cycle, after repeating the six-layer hand lay-up with 20mins settle time between each layer, the closed mould was placed inside an 80° C pre-heated oven, and slight weights were placed on top of the closed mould. After 5 hours in the oven at 80° C and allowing the part to cool down to room temperature, the composite part obtained is shown in Figure 6.15. However, the resin was still very tacky and looked like it had not been cured. Hence, the flax SBPU composite was placed back into the oven for two post-curing cycles, first at 100° C for 2 hours and second at 40° C for 6 hours. Following the two post-cure cycles, the material was not tacky anymore. However, the created flax fibre SBPU composite was very flexible and deformed by applying minimal loads with the hands. This is because of the high percentage of the soft segment in the system, which does not provide any strength for the final composite. Due to this, the manufacturing of the SBPU was put on hold, and more focus was put towards manufacturing multiple films stacked TPU-based composite.

Figure 6.13: Hand lay-up of six flax fabrics with SBPU

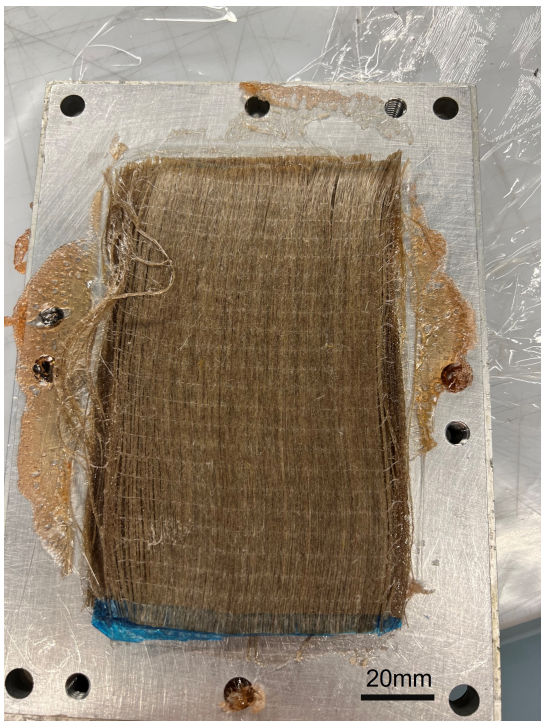

Figure 6.14: Natural fibre composite film stacked after placing under the press

Figure 6.15: Flax SBPU composite after removal from the oven

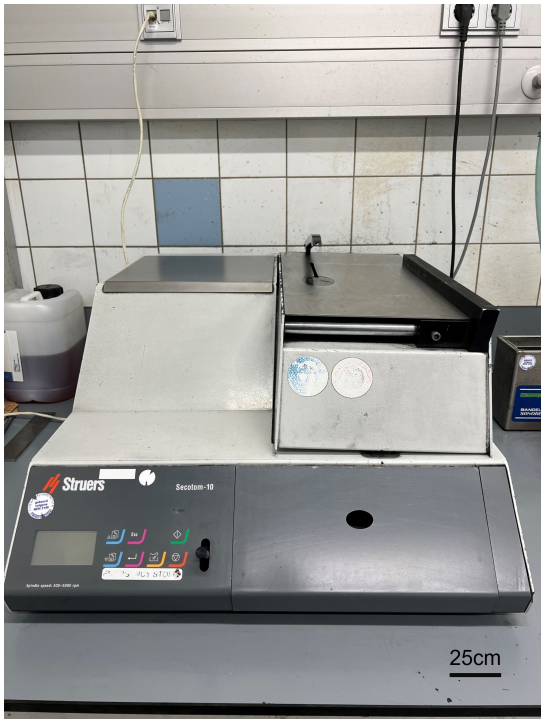

Figure 6.16: Diamond cutting machine

6.4. Sample Preparation for Testing

After preparing the composite plates, the next step is to cut them into smaller sample sizes for different tests according to the standards. As shown in Figure 6.16, a diamond cutter is used for this. The composite plates are cut into various dimensions as shown in Table 6.1 for the different tests. Additionally, the samples are placed inside an oven at 40° C after the cutting is complete. Since the diamond cutter machine uses water as a coolant, any excess moisture that could have been added to the sample after cutting must be removed. Finally, the cut samples are taken for their respective testing.

Table 6.1: Sample sizes for further testing

Testing	Specimen size (mm^2)
DMTA	30x5
Water absorption	30x30
Tensile Test	150x5
Microscopy	5x5

7

Results

This chapter includes all the tests performed on the natural fibre composite. A water contact angle test was to determine the surface wet-ability, and parallelly, a water absorption test was to understand the composite's moisture behaviour. Next, the composite's tensile and flexural test is performed to understand its mechanical properties. A DMTA study is performed to understand the influence of the fibre on matrix transition temperature and provide a result of the storage modulus of the composite. Finally, a morphological study is done on various samples to learn more about the resin interface and the fibres.

7.1. Contact angle measurement

The Sessile drop method was used to measure the advancing and receding contact angles, and the results for TPU are showcased in Table 7.1. From this, it can be noted that the mean contact angle for TPU lies in the range of 76° to 80°. Indicating that the droplets tend to wet the surface of the TPU and the resin is slightly hydrophilic. The droplets placed on the surface of the TPU can be seen in Figure 7.1. The same test was also performed for flax. However, flax is exceptionally hydrophilic and absorbs the water immediately, giving no time for an image to be captured. However, this test does not give an idea if the TPU resin absorbs the water into the system or will disperse the 8μl of water on the surface as time progresses.

Table 7.1: Water Contact angle test results for TPU resin

Resin	Trial	Contact Angle Advancing	Contact Angle Receding	Mean Contact Angle	Volume of Water Dispensed (mu l)
TPU	1	78,96	76,36	77,66	8
	2	75,84	77,62	76,73	8
	3	76,52	76,05	76,28	8
	4	78,15	77,93	78,04	8
	5	82,38	81,08	81,73	8

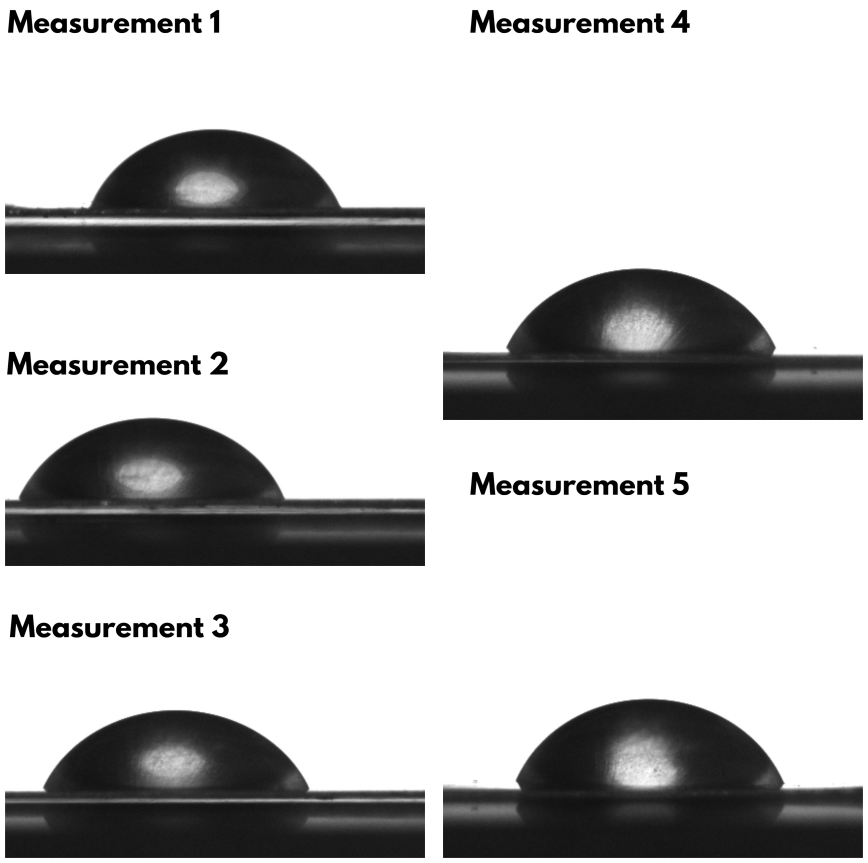

Figure 7.1: Droplet Images used for the contact angle test of TPU

7.2. Water Absorption test

After learning about the surface of the Flax/TPU, it was understood that the outer TPU layers are slightly hydrophilic. However, the water contact angle test does not indicate how much water the TPU absorbs. Therefore a water absorption test was conducted for the composite. The 30x30 mm^2 composite sample is weighed before placing it inside distilled water. The result of the experiment is showcased in Table 7.2. Here it can be seen that the Flax/TPU composite specimens' weight increased by only 17% whereas the Flax/SBPU specimen increased in weight by 129%. First, a closer look is taken at the Flax/SBPU specimen in Figure 7.3. It can be seen that in 24 hours, the colour of the solution has changed from transparent to opaque. Moreover, after having a closer examination Figure 7.5, it can be seen that the resin seems to have dispersed in the water solution causing the transparent solution to turn white. The reason for the SBPU resin dispersing in the water is due to the sugar-based acid chains present in the solvent-based polyurethane mixture. These acid groups tend to break the chains and disperse in the water. Therefore, once the resin layer is partially or entirely removed from the interface of the flax fabrics, the flax fabrics are more exposed to the water, and the flax, being hydrophilic, starts to absorb the water. The nominal thickness of the manufactured Flax/SBPU was around 2.5mm thick, but after removing from the water, the thickness seems to have doubled as seen in Figure 7.5. The reason for this size change is mainly due to the flax, as it tends to swell up due to the absorption of moisture [28]. On the other hand, the Flax/TPU specimen has a meagre increase in weight, and also, no visual changes can be absorbed in the water solution as seen in Figure 7.2. Furthermore, the specimen does not have any dimension change as illustrated in Figure 7.4. Therefore, this indicates that the manufactured sample has an excellent ability to resist any water absorption. It also means that the interface of the flax fibre and the TPU films is promising, as no layer of the flax fabric was exposed to any of the water.

Table 7.2: Water Absorption test for TPU and SBPU

Resin	Weigh of Sample before placing inside distilled water (g)	Weight of Sample After 24hrs in distilled water (g)
TPU	2.12	2.495
SBPU	3.14	7.21

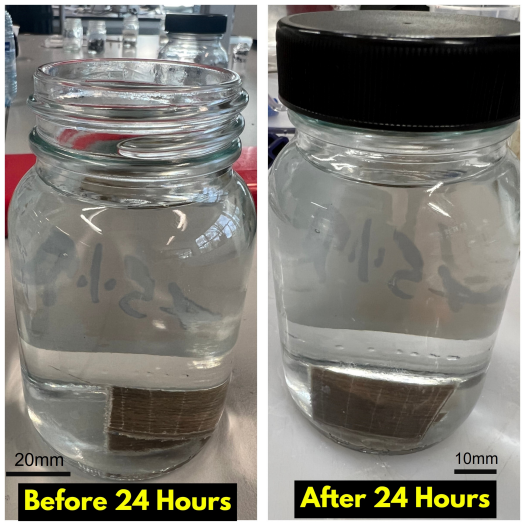

Figure 7.2: Flax/TPU Before and after 24hrs immersion in distilled water

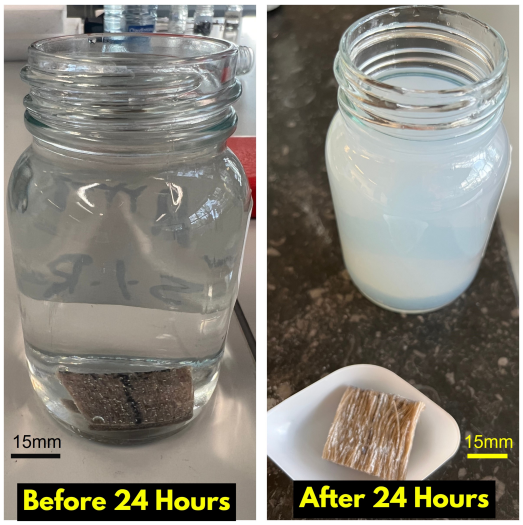

Figure 7.3: Flax/SBPU Before and after 24hrs immersion in distilled water

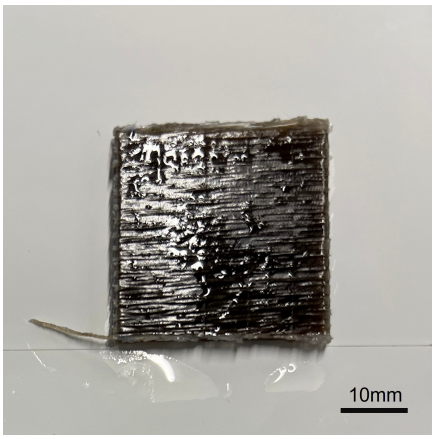

Figure 7.4: Flax/TPU after 24hrs immersion in distilled water

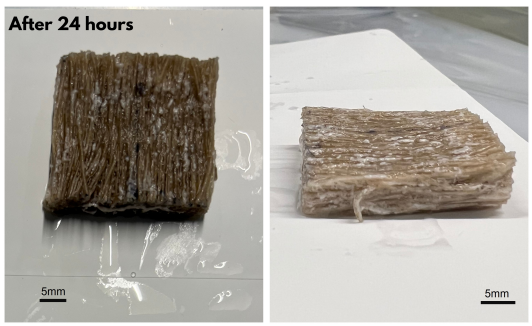

Figure 7.5: Flax/SBPU after 24hrs immersion in distilled water

7.3. Tensile Testing

A tensile test was performed to determine the strength of the manufactured material. The result of the tensile test for the resins and the composite is showcased in the sections below.

7.3.1. Resin Tensile Properties

The matrix's function is to embed the reinforcing fibres and transfer inter- and intralaminar stresses between adjacent fibres and layers. The stress-strain curves of die-cutout bulk polymers tested under uniaxial tension are shown in Figure 7.6, and all the samples are tested with a gauge length of 16mm.

The measured modulus and strength values are 3.6 MPa and 5.5MPa, respectively. All of the samples tested and failed in a brittle manner with negligible plastic deformation before rupture, as seen in Figure 7.7. All the samples failed in Mode 1 failure, and all of the samples failed in the testing region and not near the necks of the dog bone. The scattered results seen in Table 7.3 are primarily due to the varying thickness. As the resin was melted inside a Teflon mould, the property to control the thickness was unavailable. The conclusion drawn from these results is that resin is fragile due to its extremely low strength. The maximum elongation at break was observed for the sample with 2m thickness at 154%. For the future tensile test of the neat resin, it would be beneficial to try and utilize an injection moulding setup as this ensures that all the samples are consistent in cross-sectional area. The unavailability of the injection moulding machine was the reason for opting for die cutout method.

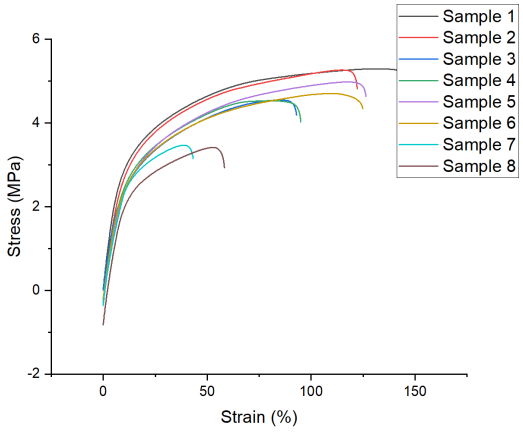

Figure 7.6: Tensile stress-strain behaviour of the TPU neat resin

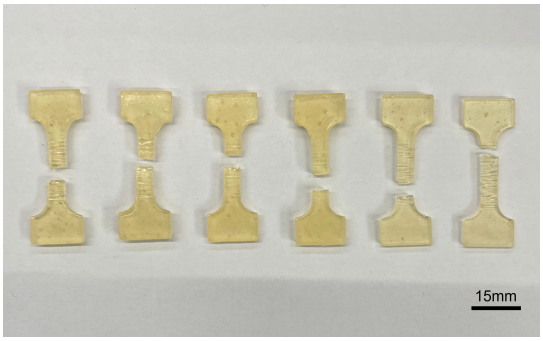

Figure 7.7: Mode 1 failure of the samples

Table 7.3: Tensile Test data foe neat resin samples

Sample	Fmax N	dL at Fmax mm	FBreak N	dL at break mm	Thickness mm	Gauge length mm	Area mm2	σ_{Max} MPa	Elongation at Break (%)
1	52.96	21.87	48.47	24.80	2.00	5	10.00	5.30	155
2	69.78	19.04	63.79	20.18	2.65	5	13.25	5.27	126
3	79.60	14.03	73.26	15.36	3.50	5	17.50	4.55	96
4	65.95	13.19	58.50	15.67	2.91	5	14.55	4.53	98
5	86.40	19.51	80.38	20.85	3.47	5	17.35	4.98	130
6	76.45	18.02	70.50	20.61	3.25	5	16.25	4.70	129
7	57.24	6.28	51.81	6.99	3.30	5	16.50	3.47	44
8	55.47	8.53	47.54	9.43	3.25	5	16.25	3.41	59

To conclude the resin has a very low strength and stiffness modulus. Indicating that in the composite most of the stiffness is provided by the flax fibre itself.

7.3.2. Tensile Testing of Natural fibre composite

After performing the tensile test on the resin, the next step is understanding the strength and modulus of the Flax/TPU composite. Looking at the results of the strength of the resin from the previous section, the resin has a very low tensile strength, and it is vital to understand how/if the flax is improving the strength of the composite system. For this first, the manufactured flax plate is cut into smaller samples of size 150mmx15mm in the 90° direction. As the sample sizes are relatively smaller, the idea is to perform a DIC, as extensometers cannot be used in the setup of the UTM due to the low gauge length. After spraying a layer of white and applying the speckle pattern, the sample was placed in the UTM between hydraulic clamps as seen in Figure 7.8. The bottom left of this image shows the sample after the test. It can be seen that resin has squeezed out from between the fibres, and the deformation has

occurred in the clamping area. The hydraulic clamp compresses the fibres causing the resin to get squeezed out and, in turn, reducing the thickness in the clamping region, ultimately causing the sample to slip out. For the next attempt, more pressure(150bar) was applied by the hydraulic clamps onto the composite, and as seen Figure 7.10 sample 2, the clamped area of the composite got compressed and slipped out once again. Hence, the idea was to change to the mechanical clamps as seen in Figure 7.9. These clams have a rougher surface area allowing for better clamping of the composite. However, after the test was concluded, it was noticed that the top and bottom layers of resin had just sheared off from the composite sample, as seen in Figure 7.10 sample 3. This is because of the low strength of the resin and is also an indication that the fibre matrix adhesion is not very strong. These three trials show that the composite cannot be compressed to a high degree and the rougher surface area clamps shear off the resin. Therefore, to solve the problems, the following approach was to use aluminium tabs in the clamping area. The surface of the aluminium tabs and the area where the tabs are placed are made rough using a sanding paper so that when the adhesive is placed in between, there can be a strong bond between the aluminium tabs and the composite. LOCTITE EA 3425 Epoxy Adhesive is the adhesive used to bond the tabs and the composite together. After applying the adhesive on the composite surface, the tabs are placed on top and clamped together with small paper clamps. This allows any excess resin to escape, and this fixture is left to sit at room temperature for 72 hours to ensure that the adhesive cures fully. After 72 hours, sample 4 Figure 7.10 is how the sample looks. This sample was placed between the mechanical clamps in the UTM and the tensile test was performed. Unfortunately, this test also failed; the aluminium tabs shear off the resin and break free from the composite sample. The reason is due to the poor strength of the resin. After four unsuccessful tests, the tensile test for the composite was put on hold. A method to try and optimize this setup would be first to do a surface treatment of the flax fibres, as this could improve the adhesion of the TPU and the flax fibre.

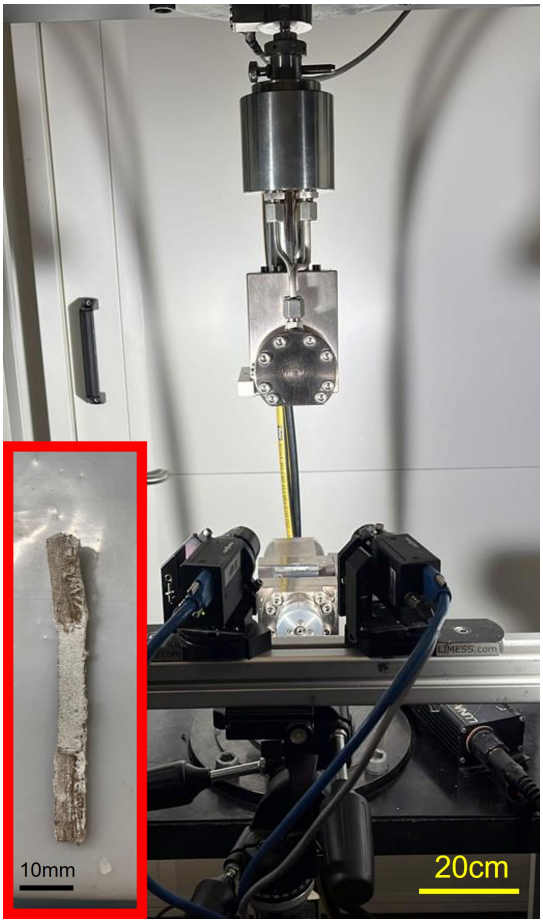

Figure 7.8: Hydraulic clamps and Tensile test failure using hydraulic clamps clamps

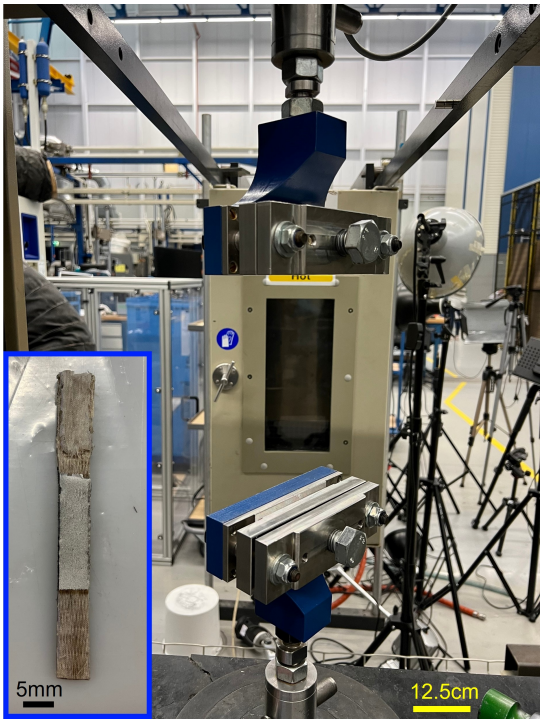

Figure 7.9: Mechanical clamps and the Tensile test failure using mechanical clamps

Figure 7.10: Result of 4 Tensile tested samples, sample 1 & 2 using hydraulic clamps, sample 3 with a mechanical clamp and sample 4 using aluminum tabs & mechanical clamps

7.4. Composite Flexural Properties

Three-point bending tests on specimens with longitudinal and transverse fibre directions were performed to characterize the role of the matrix and the interface on flexural performance. For the flexural test, samples of length 60mm and width 15mm are cut out from the manufactured Flax/TPU plate. More than five samples are needed to obtain a good data set. Once all the samples are prepared, they are placed in the 3-point bending setup as shown in Figure 7.11. Figure 7.12 illustrates the samples after the samples have been tested. A span length of 40mm was used while performing the test. A plot of Force vs deformation is achieved for all the samples Figure 7.13 and Figure 7.14 are example plots for the longitudinal and transverse direction of flax. First, the max load applied for all the samples is identified to calculate the flexural strength. Then as per ISO 14125, the formula for the calculation of the flexural strength is used, which is as follows:

$$\sigma_f = \frac{FL}{bh^2} \tag{7.1}$$

Where F is the max Load applied, L is the span length =40mm, b is the width of the sample, and h is the thickness of the sample. Following this, the flexural modulus was calculated according to ISO 14125 standard. Next, the deflection s' and s" need to be identified to do so, and these deflections correspond to flexural strain ϵ'_f and ϵ_f"; the formula used was:

$$s' = \frac{\epsilon'_f L^2}{6h} s'' = \frac{\epsilon_f'' L^2}{6h} \tag{7.2}$$

Where ϵ'_f= 0.0005 and ϵ_f"= 0,0025. Now, a slope is drawn for the region between s' and s" in the Load vs deformation plot. Finally, this obtained value of the slop is utilised to calculate the flexural modulus of the composite using the formula:

$$E_f = \frac{L^3 m}{4bh^3} \tag{7.3}$$

where m is the slope. All the calculated values are then stored together in Table 7.4 and Table 7.5.

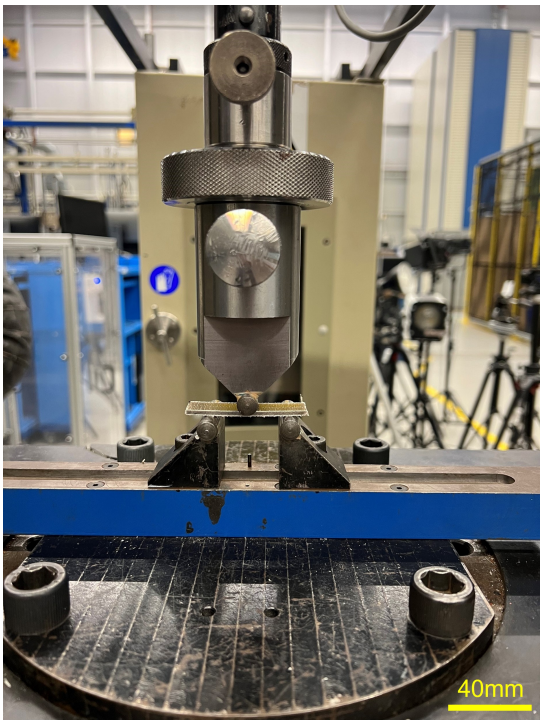

Figure 7.11: Setup for three point bending

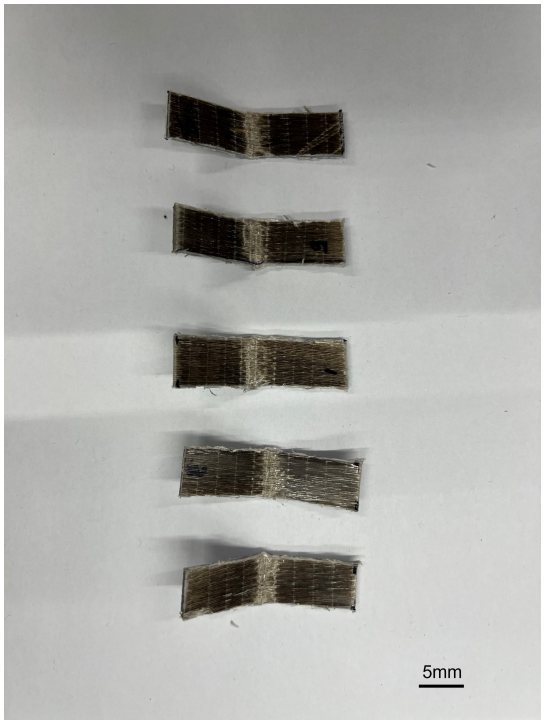

Figure 7.12: Flax/TPU samples in longitudinal orientation after the test

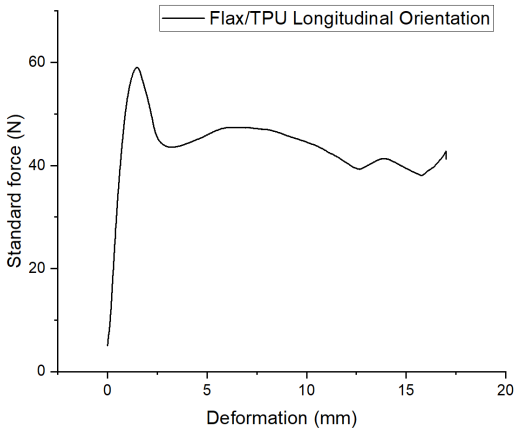

Figure 7.13: Plot of Force vs Deformation for Flax/TPU in longitudinal orientation

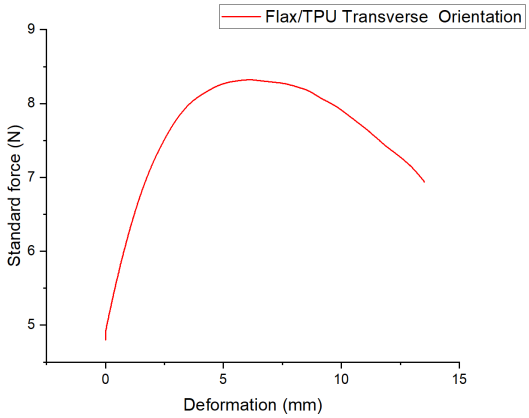

Figure 7.14: Plot of Force vs Deformation for Flax/TPU in transverse orientation

Table 7.4: Data for flexural strength and modulus calculation for Flax/TPU in longitudinal direction

Sample	Fmax [F] N	Thickness of Sample [h] mm	Width of Sample [b] mm	Flexural Strength MPa	S′ mm	S″ mm	Slope N/mm	Flexural Modulus GPa
1	63.48	1.8	15.28	76.93	0.24	1.20	40.50	7.27
2	38.82	1.8	15.28	47.05	0.24	1.20	22.84	4.10
3	53.08	1.85	14.84	62.71	0.25	1.23	44.47	7.57
4	56.44	1.83	14.07	71.86	0.24	1.22	31.06	5.76
5	36.19	1.8	8.9	75.30	0.24	1.20	22.74	7.01
6	59.03	1.8	13.7	79.80	0.24	1.20	42.08	8.43
7	58.45	1.83	14	74.81	0.24	1.22	32.87	6.13
8	58.00	1.83	14	74.22	0.24	1.22	36.40	6.79
9	61.02	1.83	14	78.09	0.24	1.22	38.21	7.13
10	55.40	1.83	14	70.90	0.24	1.22	33.52	6.25
11	63.21	1.9	14.9	70.50	0.25	1.27	38.87	6.09
12	56.43	1.88	15	63.86	0.25	1.25	35.11	5.64

Table 7.5: Data for flexural strength and modulus calculation for Flax/TPU in transverse direction

Sample	Fmax [F] N	Thickness of Sample [h] mm	Width of Sample [b] mm	Flexural Strength MPa	S′ mm	S″ mm	Slope N/mm	Flexural Modulus MPa
1	7.32	2.04	14.94	7.06	0.07	0.33	1.48	186.07
2	7.47	2.04	14.94	7.21	0.07	0.33	1.86	235.01
3	6.31	2.04	14.94	6.09	0.07	0.33	0.90	113.28
4	8.29	2.18	15.44	6.78	0.06	0.31	2.22	221.79
5	8.40	2.15	15.18	7.19	0.06	0.31	2.20	233.02
6	7.11	2.05	15.84	6.40	0.07	0.33	1.38	162.19
7	7.68	2.25	15.5	5.87	0.06	0.30	1.66	150.59
8	7.38	2	15.66	7.07	0.07	0.33	1.48	189.28
9	8.33	2.3	15.33	6.16	0.06	0.29	1.62	138.55

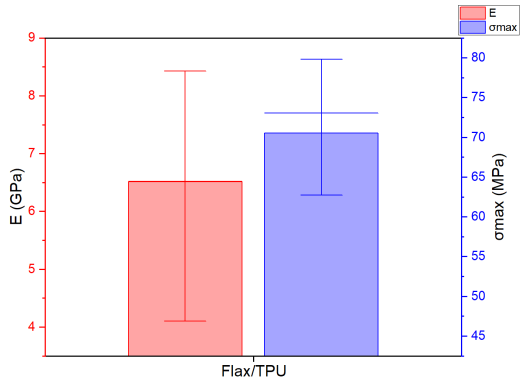

Figure 7.15: Flexural properties of flax fibre reinforced composites: Modulus (red bar) and strength (blue bars) in longitudinal direction

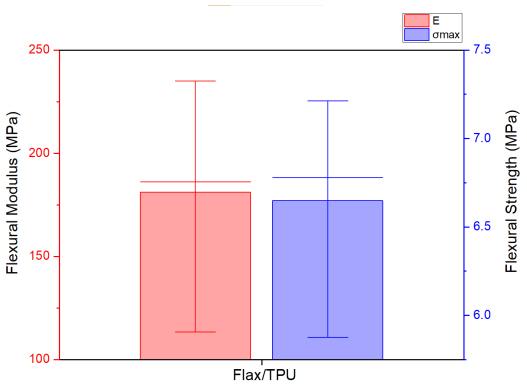

Figure 7.16: Flexural properties of flax fibre reinforced composites: Modulus (red bar) and strength (blue bars) in transverse direction

Finally, the flexural strength and moduli values are plotted in a box graph and depicted in Figure 7.15 and Figure 7.16. The measured flexural moduli (red bar) and strength values (blue bar) for longitudinal and transverse directions, respectively. From the graphs, it can be noted that Flax/TPU in the longitudinal direction have an average flexural strength of 70.5 MPa and a flexural modulus of 6.51 GPa. And as expected a much lower flexural strength of 6.65 MPa and a flexural modulus of 181 MPa in the transverse direction.

7.5. Dynamic mechanical analysis(DMA)

The modulus and tan delta values are the results of DMA's measurement of stiffness and damping, respectively. The elastic properties of a sample are quantified by its storage modulus, which might be either E′ or G′. Damping is defined as the ratio of the loss to the storage, or tan delta. To determined the stiffness property of the composite and to understand the phase transition of the resins, a DMTA test is performed on the Flax/TPU composite. A sample size of 30mm x 5mm is used for this test. After placing the sample inside the DMTA machine, a temperature sweep is performed on the sample from a temperature of -100° C to 50° C. The graph of loss modulus, storage modulus, and tan (delta) vs temperature is illustrated in Figure 7.17. Here it can be seen that around the temperature of -50° C to -35° C, there is an increase in the value of Tan(delta) & loss modulus and a drop in value in the storage modulus. This is an indication of the glass transition temperature of the material. From the DSC of the resin, it is known that the T_g of the soft segment lies in this region. Also. The next change in loss modulus and tan (delta) can be observed around 40° to 60°. Also, from the DSC of TPU, it is known that this is the T_g of the hard segment of the TPU. Additionally, the storage modulus as seen in Figure 7.17 showcases a value of 3.3GPa. Which represents that the material has stiffness of 3.3GPa. In conclusion a approximate value of stifness for the Flax/TPU same was achieved with DMTA and it also showcases that the fibres do not alter any of the transition temperature of the resins after the composite was manufactured.

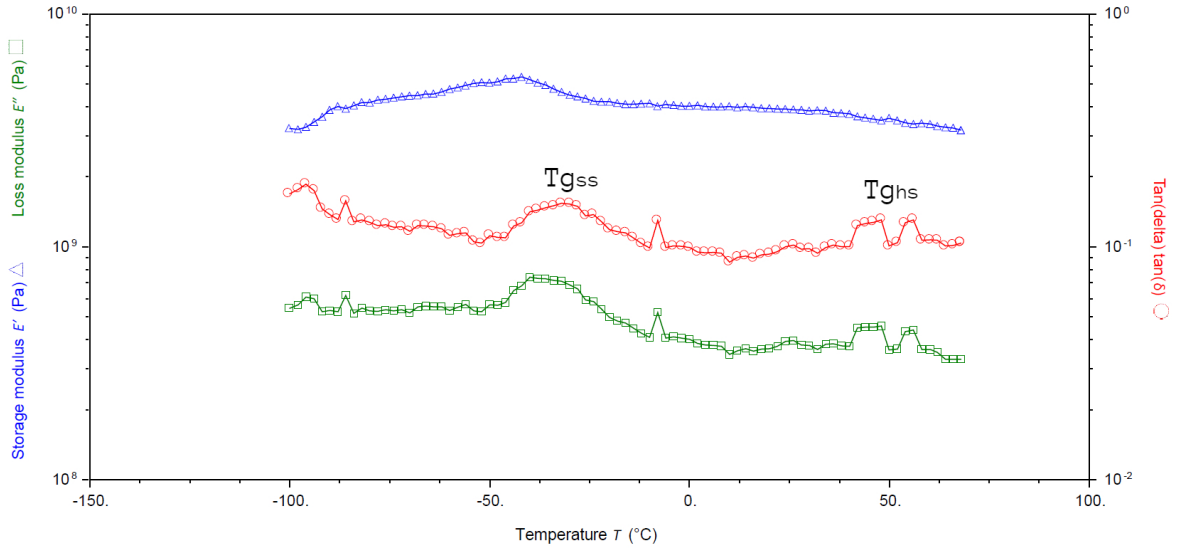

Figure 7.17: Dynamic mechanical analysis result of Flax/TPU composite

7.6. Microscopy and image analysis

The composite morphology was studied using cross-sectional image analysis to assess impregnation quality. The prepared sample was placed on the Keyance laser microscope, and as mentioned in the methodology, there were three samples prepared for viewing 1. Flax/TPU composite 2. Flax/SBPU composite, and 3. The interface of Flax/TPU composite after the tensile test.

The Flax/TPU composite is observed; first, two images with two different magnifications are recorded for this composite. First, an image of the entire cross-section is captured with 2x magnification as seen in Figure 7.18. Here it can be noticed that the out layers of the composite are perfectly straight, and there are no irregularities on the outer layers. It also indicated that the thickness across the cross-section of the sample remains the same. Next, to have a closer look at the fibre matrix interface, the sample is viewed at 25x magnification as seen in Figure 7.19. Here, it can be seen that the impregnation resulted in consistent fibre volume fractions and relatively low porosity in the NF-composites.

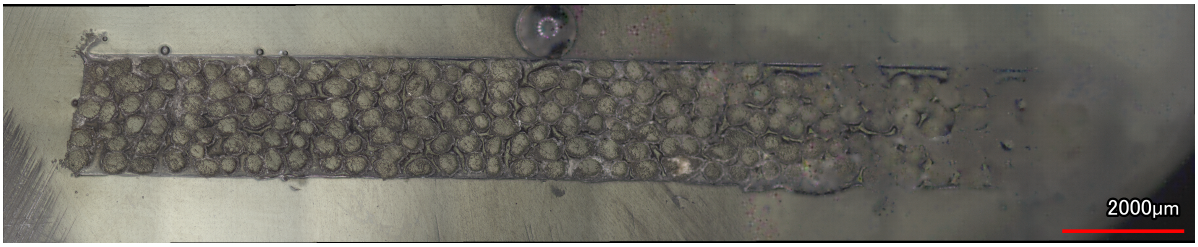

Figure 7.18: Morphology of the Flax/TPU composite at 2x magnification

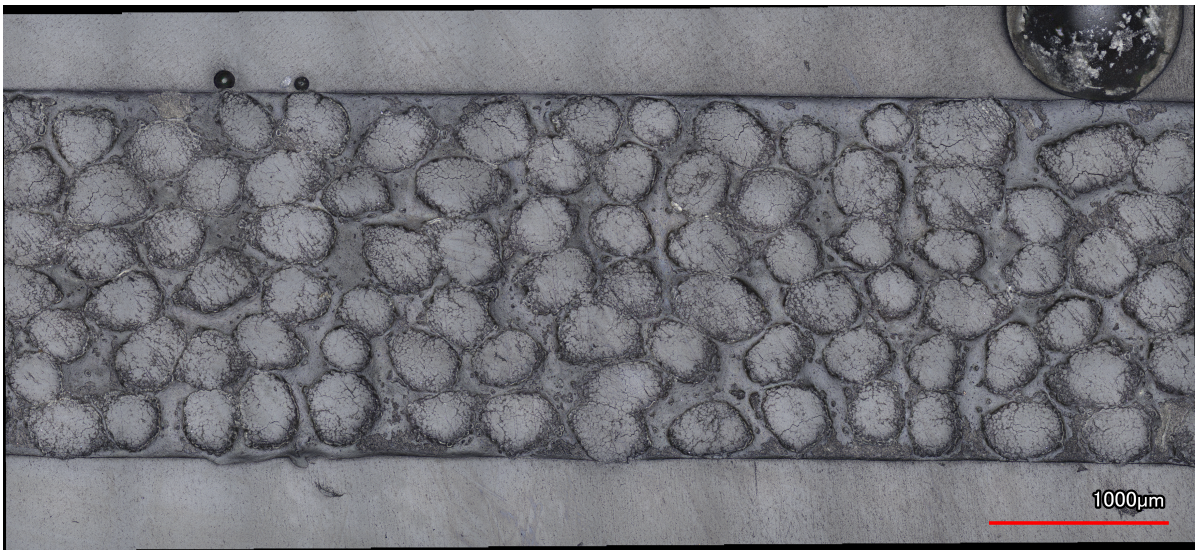

Figure 7.19: Morphology of the Flax/TPU composite at 25x magnification

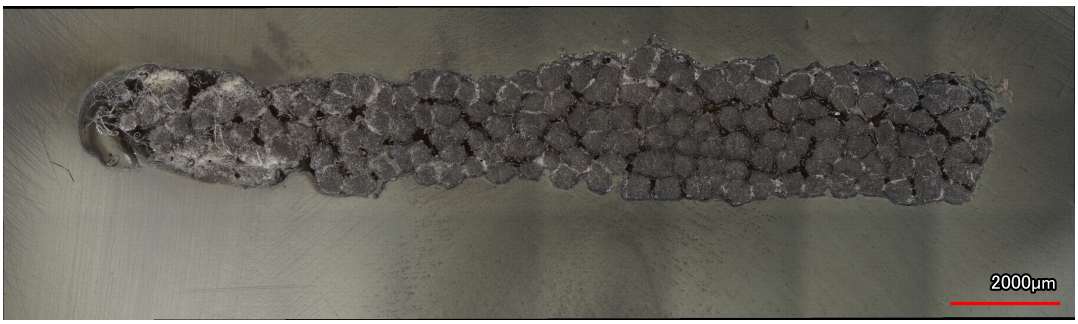

Figure 7.20: Morphology of the Flax/SBPU composite at 2x magnification

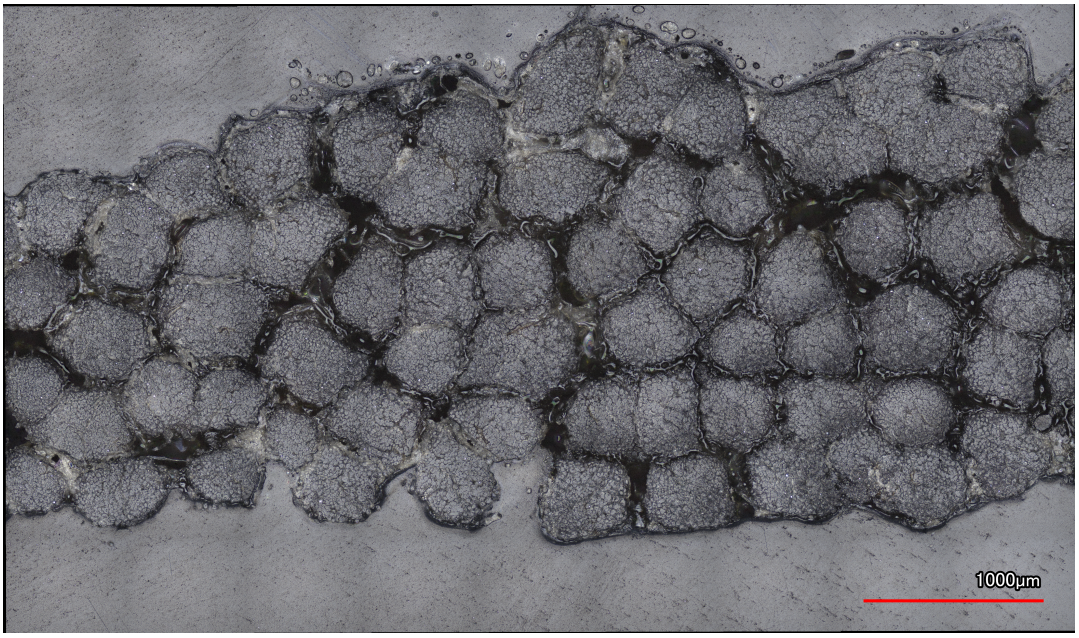

Figure 7.21: Morphology of the Flax/SBPU composite at 25x magnification

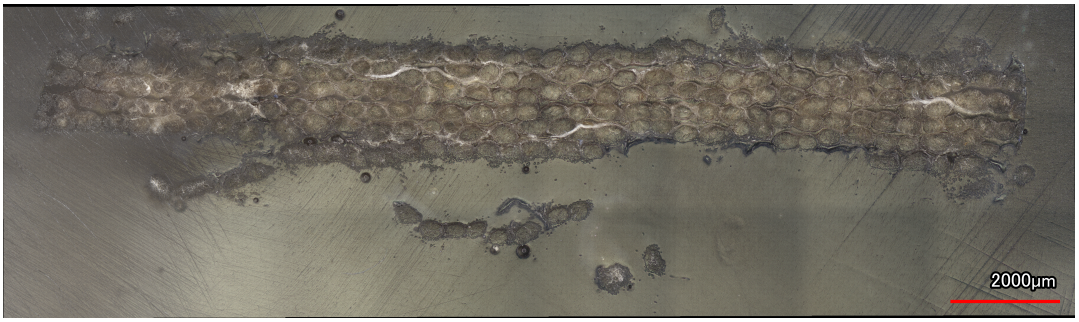

Figure 7.22: Morphology of the Flax/TPU composite after tensile testing at 2x magnification

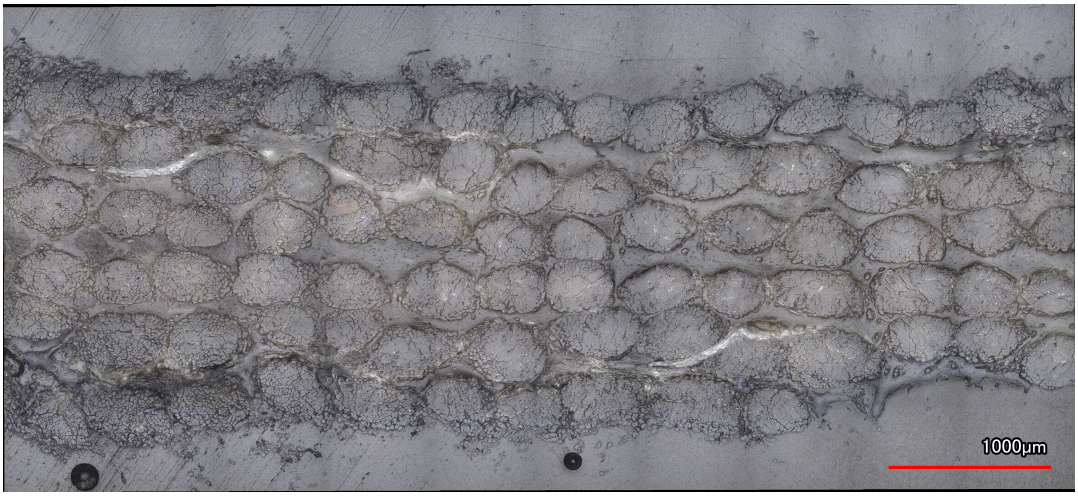

Figure 7.23: Morphology of the Flax/TPU composite after tensile testing at 25x magnification

The Flax/SBPU composite is viewed next; similar to the TPU, the sample is the view under two magnifications, 2x and 25x. The 2x magnified image can be seen in Figure 7.20, and it can be noticed very quickly that the sample thickness varies across the cross-section. The number of flax fabric layers on the left of Figure 7.20 seems to be comparatively less than that of the right side. The reason for this could be due to the handling of the flax/SBPU plate. As motioned earlier, due to the high content of soft segment chain in the solvent-based polyurethane, the manufactured composite is very soft, and a slight application of load by hand could have deformed the plate. To understand the interface of the resin and the fibres, the sample is viewed at a magnification of 25x, as seen in Figure 7.21. From this image, it is pretty clear that the fibre volume fraction is very high as many voids can be observed between the fibres, and in some regions, there are fibres bundled together with no resin. Therefore, the Flax/SBPU showcases a low resin content and is tricky to handle due to being very soft.

Finally, the failed interface of the Flax/TPU composite tested for tensile with the mechanical clamps is also observed under the microscope. Figure 7.22 is the magnification of the sample in 2x, and from this, it can already be seen that the top and bottom layer of TPU has sheared off the composite. On the left side of the Figure 7.22, it can also be noticed that a few layers of flax fabric and resin have also sheared off. A closer look is taken into this sample with 25x magnification, and as seen in Figure 7.23, it is obvious now that the top and bottom layers of TPU have entirely been removed. Also, the spacing between two fabric layers seems to have reduced compared to the untested Flax/TPU sample. This could be due to the clamping pressure applied on the sample, causing the resin to squeeze out and the fabric layer to get pushed close. In the future, a treatment could be performed on the flax fabric to bond better with the TPU matrix.

To conclude, a consistent fibre volume fraction is achieved in the Flax/TPU composite. However, the same cannot be said for the Flax/SBPU composite, which showcases a very low resin content in the composite structure and a very poor cross-section with varying thicknesses. Finally, the morphological interface of the tensile tested sample of the Flax/TPU confirms that the resin outer layers have been completely sheared off.

8

Life Cycle Assement

8.1. Goal

This study aims to assess the environmental impact of the production of Flax/TPU biocomposite laminates (150 x 90 mm^2) using ISO 14044 methodology. The main criterion to identify is the amount of carbon dioxide embodied vs a traditional polyurethane polymer.

8.2. Scope of the study- System boundaries

Life cycle analysis must be performed for a well-defined data set, as the ISO 14044 standard recommends. Figure 8.1 depicts the study's limits for Flax/TPU biocomposites. Boundaries include component production and associated emissions (air, water, soil), film production and composite manufacturing. Because of the apparent lack of data on the waste treatment of biocomposites, the study is limited to a Cradle to Gate approach.

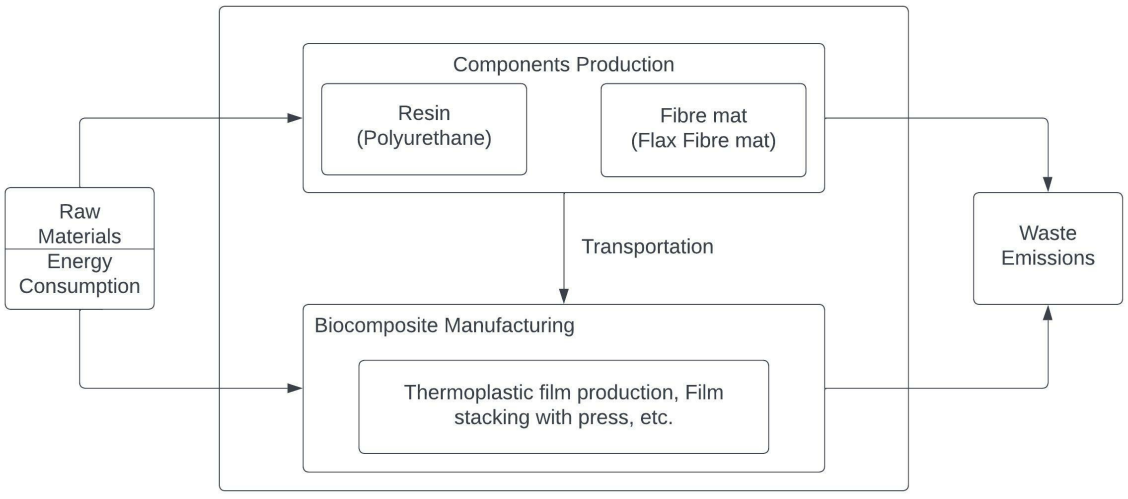

Figure 8.1: System boundaries for Flax/TPU natural fibre composite

8.3. Embodied Carbon dioxide

One of the main goals of the research is to calculate the embodied carbon dioxide present in the Flax/TPU composite. As the polyol in the TPU resin is of bio origin, it is compared against a conventional/commercial polyol. The process for the creation of the natural fibre composite first begins with the extraction of flax. From the literature, it is known that flax captures 1.38kg of CO_2 per kg of flax

[39]. Moreover, according to the datasheet provided by BComp, 1.65 kg of CO_2 sequestrated / kg of flax fibre. Polyurethane is created using two main precursors, polyol and isocyanates. Conventional polyol has an embodied CO_2 of 3.57 kg of CO_2 per kg of polyol produced [2]. In this thesis, the polyol used had a bio-based origin from algae. From [38], it is found that algae capture 1.8 kg of CO_2 per kilogram of algae biomass. Furthermore, as no exact value of embodied CO_2 can be calculated for the algae-based polyol, an assumption is made that the embodied CO_2 for the algae-based polyol is 1.77 kg of CO_2 per kg of polyol produced due to the origination from bio-source. Also, as algae capture CO_2, the net CO_2 for this system will be considerably lower than that of the conventional polyol setup. The diisocyanate used for both systems comprises 2.313 kg of CO_2 per kg of Methylene diphenyl diisocyanate (MDI), and finally, for the processing of the composite, knowledgeable assumptions is made of 1kg of CO_2 per Kg of Flax/TPU plate. All the data is listed in Table 8.1. Figure 8.2 shows a graphical representation of the embodied carbon dioxide in different stages of the natural fibre composite.

Table 8.1: Data of embodied CO_2 for all the stages of preparation of Flax/PU

	Starter (kg per CO_2 eq)	Utilities (kg per CO_2 eq)	Epoxides (kg per CO_2 eq)	CO_2 Source (kg per CO_2 eq)	Raw material (kg per CO_2 eq)	Processing (kg per CO_2 eq)
Flax					-1.38	
Flax Fibre						1.69
Conventional Polyether polyol	0.25	0.25	2.5	0.57		
Algae Biomass					-1.8	
Algae Based Polyol	0.25	0.25	1	0.27		
MDI						2.131
Composite manufacturing						1

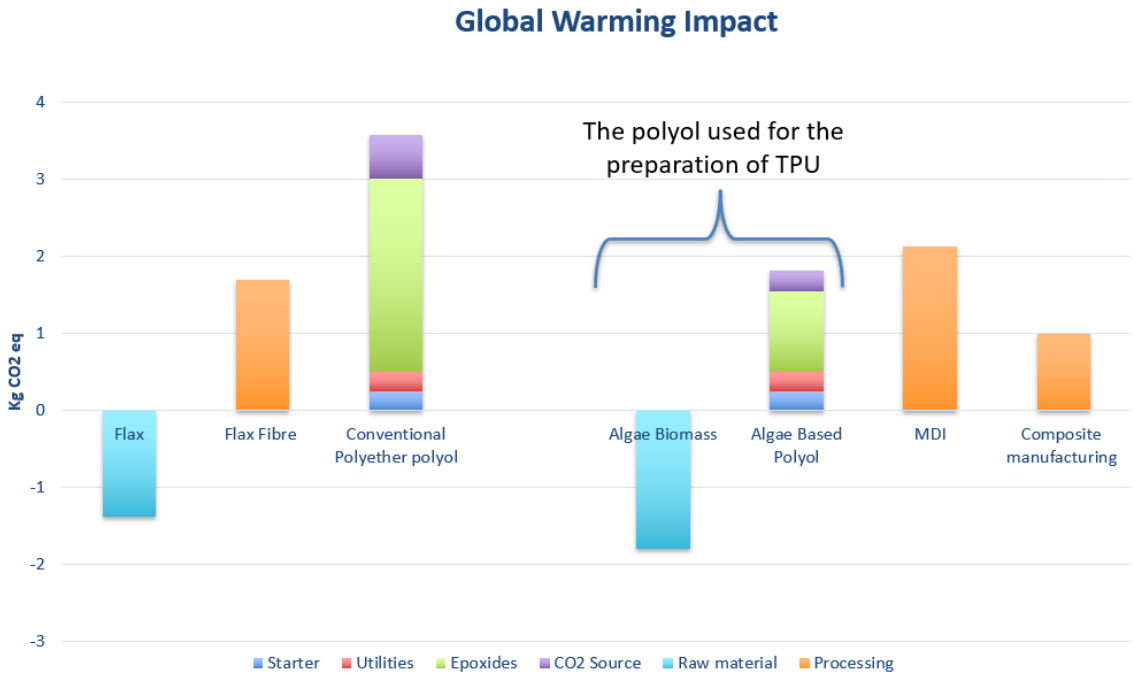

Figure 8.2: Breakdown of embodied CO_2 in all stages

Figure 8.3, is a representation of the total CO_2 embodied in the Flax/TPU composite. Data of the embodied carbon in various stages can be seen in Table 8.2. From this data, the conventional polyol composite produces about 7kg CO_2 per kg of Flax/TPU, whereas the CO_2 embodied in the algae-based Flax/TPU is about 6.5 kg of CO_2 per kg of Flax/TPU. However, this value is reduced considerably due to the carbon dioxide-capturing nature of flax and algae, and a value of 3.4 kg of CO_2 per kg of Flax/TPU is achieved. Implying that the algae-based Flax/TPU is much more sustainable than the conventional one. Also, for the future, the same group in UC San Diego are preparing a diisocyante made out of algae origin, which can replace the currently used MDI in the Flax/TPU system, thereby further reducing the embodied CO_2 of the system.

Table 8.2: Break down of total embodied carbon in Flax/TPU and Flax/Conventional PU structure

	Flax Plant (kg CO_2 eq.)	Flax Fibre (kg CO_2 eq.)	Algae Biomass (kg CO_2 eq.)	Polyol From Algae (kg CO_2 eq.)	Conve-ntional Polyol (kg CO_2 eq.)	MDI (kg CO_2 eq.)	Composite Manufa-cturing (kg CO_2 eq)	Total Embodied CO_2 (kg CO_2 eq.)
Flax/TPU Algae Based	-1.38	1.69	-1.8	1.77		2.131	1	**3.4**
Flax/TPU conve-ntional	-1.38	1.69			3.57	2.131	1	7

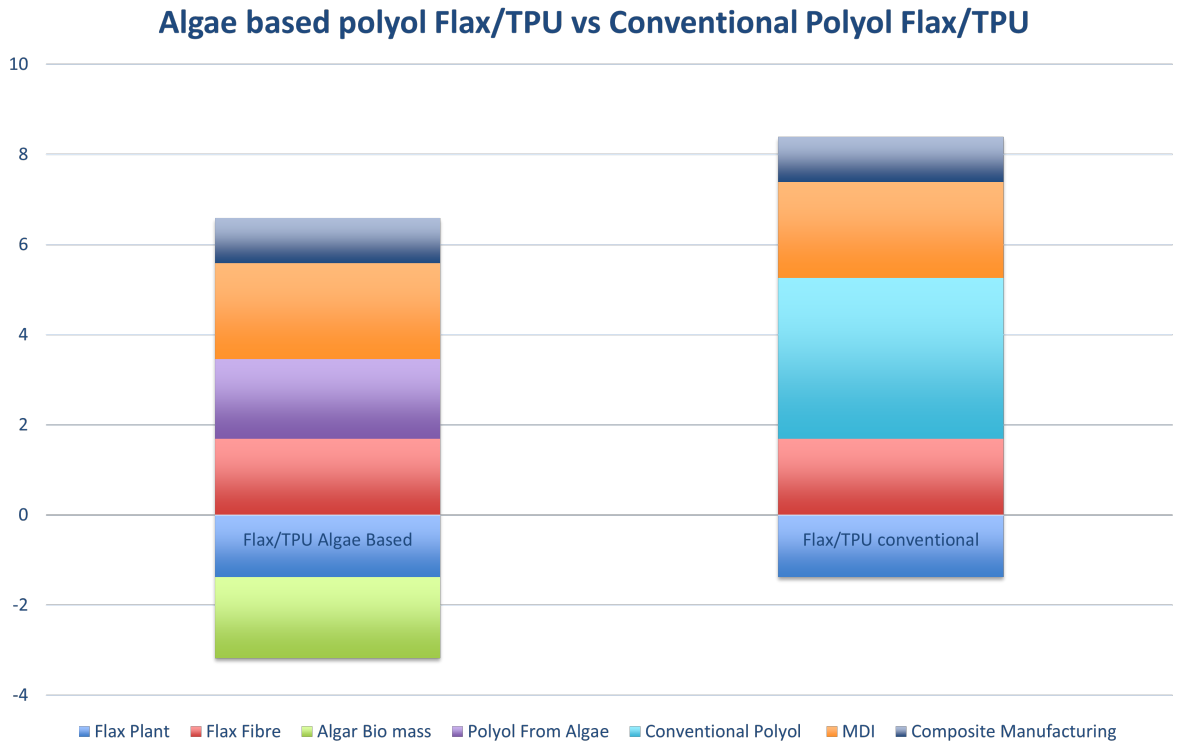

Figure 8.3: Comparision of embodied CO_2 in bio-based TPU vs conventional TPU

Additionally, since inspiration is taken from Woigk's work, a study compares the embodied CO_2 of Woigk's work and the Flax/TPU. The resin used in the work were epoxy, polypropylene (PP), poly-l-lactide (PLLA) and polyoxymethylene (coPOM). After reviewing various literature papers, values for their respective CO_2 emission are noted and written in Table 8.3. Also, a graph representation of each resin embodied CO_2 is illustrated in Figure 8.4.

Table 8.3: Data of embodied CO_2 of the resin used in Woigk's work obtained from other literature sources

	Raw material (kg CO_2 eq.)	Processing (kg CO_2 eq.)	Embodied CO_2 (kg CO_2 eq)	Database
Flax	-1.38			[39]
Flax Fibre		1.69		BComp datasheet
PP			1.6	[1]
Epoxy			6.7	[8]
PLLA	-1.833	1.333	0.5	[14]
coPOM			3.2	[17]

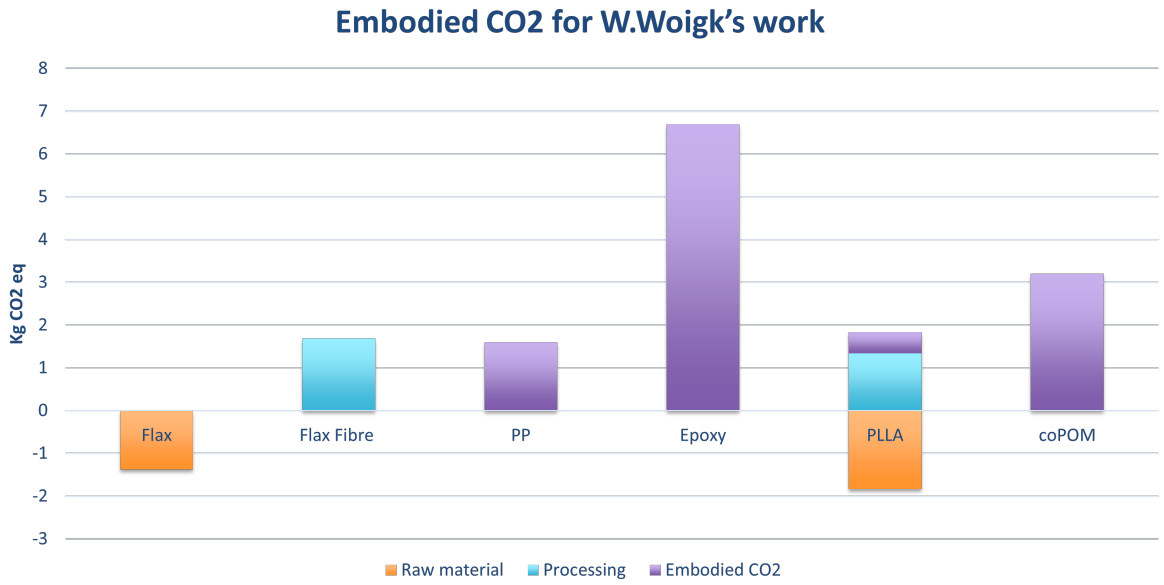

Figure 8.4: Data of embodied CO_2 of the resin used in Woigk's work

The goal is to plot a CO_2 embodied vs density curve and Young's modulus vs density curve for these six materials (Flax/TPU, Flax/PU(conventional), Flax/PP, Flax/Epoxy/ Flax/PLLA and Flax/coPOM) created. Using the rule of mixtures, the density for the composite and Young's modulus for the composite is calculated. The following formulas are used:

$$\rho_{composite} = \rho_f v_f + \rho_m v_m \tag{8.1}$$

Where $\rho_{composite}$, ρ_f, ρ_m, v_f and v_m are the density of composite, density of fibre, density of matrix, fibre volume fraction and matrix volume fraction, respectively. Similarly, the rule of mixture to calculate stiffness is as follows:

$$E_{composite} = E_f v_f + E_m v_m \tag{8.2}$$

where $E_{composite}$, E_f, E_m, v_f and v_m are Young's modulus of composite, Young's modulus of fibre, Young's modulus of the matrix, fibre volume fraction and matrix volume fraction, respectively. For both calculations, a fibre volume fraction of 50% is considered. The stiffness and density data for the different resins and flax fibre are found through various literature and noted in Table 8.4. After applying the rule

of mixture formulas for each resin, the calculated values of composite densities and Young's modulus are noted in Table 8.5. To calculate the embodied CO_2. Data from Table 8.2 and Table 8.3 are used to calculate the total embodied CO_2 for each composite. Finally, a plot of embodied CO_2 vs density of these materials is plotted as shown in Figure 8.5, and from this, it can be seen that the Flax/TPU composite has much lower embodied CO_2 when compared to petroleum-based epoxy and conventional PU. However, the Flax/PLLA has the lowest embodied CO_2 due to its origin from sugarcane and much lower CO_2 emission during processing when compared to the Flax/TPU that was created during the thesis. Next, a plot of Young's modulus vs density is illustrated in Figure 8.6. Here the Flax/TPU created in the thesis showcases the lowest stiffness due to the weak PU matrix, and Flax/PLLA showcases the high stiffness.

Table 8.4: Density and stiffness values of flax fibre and different resins

Material	Volume Fraction	Resin Fraction	Density	Stiffness
	Vf	Vr	g/cm^3	GPa
Flax	0.5	0.5	1.5	52.6
PU from Algae-Based Polyol	0.5	0.5	1.14	0.03
Conventional PU	0.5	0.5	1.47	0.021
PP	0.5	0.5	0.91	1.325
Epoxy	0.5	0.5	1.1	3.42
PLLA	0.5	0.5	1.24	4.8
coPOM	0.5	0.5	1.41	2.5

Table 8.5: Flax/resins density and stiffness calculation using the rule of mixture and Calculation of embodied CO_2 using data from literature

	Density of Composite	Embodied CO_2	Stiffness of Composite
	g/cm3	kg CO_2 eq.	GPa
Flax/PU from Algae-Based Polyol	1.32	3.4	26.31
Flax/Conventional PU	1.485	7	26.31
Flax/PP	1.205	1.91	26.96
Flax/Epoxy	1.3	7.01	28.01
Flax/PLLA	1.37	0.81	28.7
Flax/coPOM	1.455	3.51	27.55

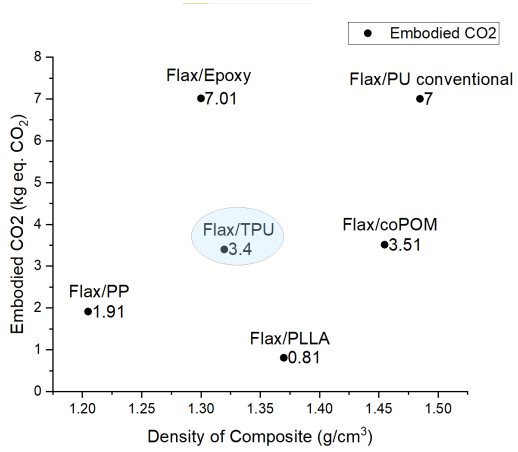

Figure 8.5: Embodied CO_2 vs Density curve for the six different materials

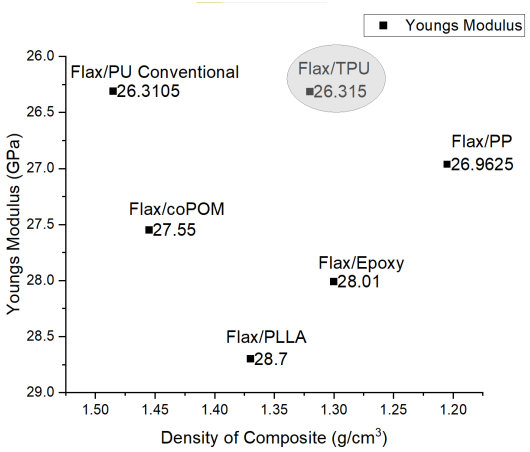

Figure 8.6: Young's Modulus vs Density curve for the six different materials

In conclusion, a basic LCA is performed on the manufactured Flax/TPU plate, and only one impact category is assessed. Which is to understand the embodied carbon dioxide in the system. After performing a fundamental analysis by gathering data from relevant literature, a value of 3.4 kg of CO_2 per kg of Flax/TPU can be expected from the product. These low CO_2 emission values are because of the carbon dioxide-capturing bio sources. Also, after comparing the data with the materials used in Woigk's work, Flax/PLLA is a very promising material as it not only proves to have high stiffness but also showcases the lowest amount of embodied CO_2. Nonetheless, once the diisocyantes used for polyurethane are prepared using a bio-source, the embodied CO_2 value for the Flax/TOU composite will also reduce drastically.

9
Outlook

9.1. Conclusion

The Burkart group at UC San Diego created a novel polyol derived from an algae biomass and this polyol is a precursor for the production of Polyurethane. However, this material lacked characterization and had not been used to produce a composite. With sustainability in mind, the plan was to manufacture a natural fibre composite using these alage derived resin. Whilst also identifying the amount of carbon dioxide embodied in the structure. The Polyurethane was provided in the form of pellets and a solvent-based. The research commences with characterizing both these materials. After performing rheology, the melt viscosity was obtained for both resins. The results of SBPU resin showcased a constant decrease in viscosity from a low temperature, owing to the solvent present in the mixture. The TPU showed a significant change in viscosity at a temperature of 110° C, which led to the conclusion that 130° should be used as the processing temperature for further experiments. During the thermal stability test performed using TGA, it was found that the SBPU resin had a considerable loss in weight due to the solvent present in the structure. At the same time, the TPU was fully stable up to a temperature of 270° C, beyond which it started to decompose. A DSC measurement was performed to understand the different transition temperatures of the resins. The TPU resin showcases two T_gs, one for the soft segment and one for the hard segment, while the SBPU resin is only displayed on T_g for the soft segment. This is due to the meager percentage of hard segment chains in the structure. The thermal characterization showed that the SBPU was not very stable for preparing composite materials. Hence, more emphasis was placed on the TPU pellets.

Upon understanding the thermal properties of the TPU resin, a pressure-temperature cycle was prepared to produce uniform void-free polyurethane films. These films were then staked alternatively with layers of flax fabrics to produce the Flax/TPU composite. The composite showcased a longitudinal flexural strength of 70.5 MPa and a longitudinal flexural modulus of 6.51 GPa. In the transverse direction, a much lower flexural strength of 6.65 MPa and a flexural modulus of 181 MPa. When compared to the work of W.Woigk et al. [41], who worked with thermoplastics Matrix materials, such as poly-l-lactide (PLLA) and co-polyoxymethylene (coPOM), which exhibit epoxy-like bulk properties, according to the findings, the longitudinal modulus and strength of PLLA matrix NF-composites were 27 GPa and 308 MPa, respectively. In the stronger coPOM matrix NF-composites, both transverse stiffness and strength were relatively high (2,6 GPa and 41,5 MPa, respectively). The Flax/TPU manufactured is much weaker than the other materials mentioned in Woigk's work. However, they have the edge over other thermoplastic resins due to their bio-based source, which is a carbon-capturing material.

Finally, a rudimentary LCA is performed to analyze the amount of carbon embodied in the structure. As the TPU utilizes an algae-derived polyol, it was compared to a conventional/commercial polyol. This showed that the TPU utilized in this thesis is much more sustainable than the conventional PU, emitting 3.4kg CO2 per kg of FLax/TPU compared to the 7.5kg CO2 for the conventional PU.

This study demonstrates that thermoplastic polyurethane polymers are appropriate matrices for natural fiber-reinforced composites. By studying the bulk properties, applying appropriate processing conditions such as compression moulding in a closed mould, and using surface energy analysis to evaluate the spreading of the polymer on the fibre and the interface strength in the composite, it is

possible to design high-performance thermoplastic composites reinforced with natural fibres. The findings of this study will aid in driving the applications of NFC towards structural components, demonstrating circularity and a reduced ecological footprint. And they have significant relevance in the emerging field of high-performance materials derived from renewable resources.

10

Future Scope

10.1. Limitations

There are two main limitation that were observed after concluding the thesis. First, the multiple iterrative failures during the tensile test was an indication that the adhesion between the fibre and the resin was poor. One reason could be due to the natural fibres. The use of natural fibres for traditional reinforcing materials in polymer composites has gained widespread acceptance. However, due to their poor interaction with polymeric matrix, the hydrophilicity of natural fibres is a significant disadvantage as reinforcements. Therefore, their surfaces must be treated for them to be employed as composite reinforcements more easily. The goal should be to determine how changing the surface of the fibre affects the performance of the composites. In an experiment performed by Umit et al. [20] the surface of the flax fibre was treated with acetic anhydride, sodium hydroxide, and silane. Contact angle, attenuated total reflectance-Fourier transform infrared, atomic force microscopy (AFM), and scanning electron microscopy tests were performed to investigate the fibre and its response to the treatments. Analyzing the contact angle and employing the AFM revealed that the adhesion force on the fibre surface of flax fibres treated with sodium hydroxide was greater. The NaOH treatment improved the mechanical properties of the epoxy matrix composite in particular. Therefore, similar chemical treatments could be performed on the flax fabrics and a surface treated Flax/TPU composite can be created and tested for adhesion and various mechanical properties.

The next limitation was the low amount of resin supplied by the supplier as more resin could have helped in manufacturing more samples. More samples to test help in providing better statics of the data collected. Also, the plat sizes wouldn't have been restricted to 150 x $90mm^2$. As creating larger plates would have enabled to use of the best tensile testing machine available in the aircraft hall, the Zwick 250KN machine. Additionally, more samples with different fibre orientations could be created. This thesis limited itself to only $[90]_6$ and $[0]_6$ Flax/TPU plates. However, many of the material's mechanical properties for different orientations might be achieved by the application of a combination of conventional lamination theory and modified principles of mixture. With this information, various Flax/TPU composites with optimised characteristics can be produced.

10.2. Future research objectives

There were two interesting research areas that could help improve the mechanical property of the natural fibre composite. First, would be the addition of additives into the TPU mixture, this could help in improving certain properties of the NFC. Next, is delignification of the flax fibres. This is due to the fact that delignification makes it easier for polymers to infiltrate the cellular walls of wood.

10.2.1. Additives

When attempting to improve the performance of polymeric composites by selecting appropriate filler materials, scientists have recently encountered substantial barriers. As a result, a great deal of emphasis has been made on enhancing polymeric composites by using nano fillers. Nano reinforced particle' polyester matrix composites (PMCs) are widely employed in the industrial industries due to their

superior fracture toughness, low weight, high strength-to-weight ratio, high tensile characteristics, high fatigue resistance, and enhanced corrosion resistance to harsh environments. Mahmoud Yousry et. al [29] examine how PMCs are constructed and the numerous reinforcements they contain. In the study cotton, banana, jute, kenaf, coir, hemp, and sisal are some of the natural fibres utilised in polyester composite materials. It discusses nano particles including nano clay, carbon nanotubes, nano graphene, and nano graphene oxide. Separate and combined evaluations of the studied material systems that, when combined, produce polyester nanocomposites demonstrate their individual and collective scientific progress. The studies major objective is to give empirical evidence linking the quantity of reinforcement used to processing-induced increases in general mechanical properties such as tensile, compression, fatigue, hardness, and flexural strength, etc. The work then concludes by stating that manufactured material has a high elongation, electrical conductivity, and strength-to-weight ratio. Incorporating filler material into the current TPU may prove interesting as the resins showcases a very low tensile strength which could benefit from these additives.

10.2.2. Delignification

M. Frey et. al [11] disscuss the delignification of Wood–Polymer that exceed the charecteristics claculated by rule of mixture. Wood is a material of increasing attention in the development of sustainable structural materials due to its hierarchical structure, which includes an oriented reinforcing cellulose phase, carbon sequestration, and renewability. With direct access to this hierarchical cellulose scaffold, new functional materials can be created using top-down production processes. To generate high-performance, load-bearing wood-based composites, the fibre volume content (FVCs) of the reinforcing phase must be greatly increased . Densification followed delignification, which kept the original structure of the wood. Due to the conservation of hierarchical fibre alignment, the matrix-free materials created have great tensile stiffness, but they have poor mechanical properties in bending and cannot be used in wet settings. Researchers have developed a composite material with interpenetrating wood polymer phases, with an epoxy resin matrix and a delignified wood scaffold functioning as the continuous reinforcing phase, to fight these difficulties. The open, continuous porosity of delignified wood enables us to employ a vacuum to permeate a matrix into the wood's structure in a manner that would be impossible otherwise. Before the matrix is cured, the wood scaffold is densified in order to increase the FVC, decrease the porosity, and standardise the density. Due to the compressibility of delignified cellulose fibres, interpenetrating phase composites (IPCs) with FVCs of up to 80% can be made, resulting in unusually high tensile stiffness and strength of up to 70 GPa and 600 MPa, respectively. Because of the stiffness-supplying matrix phase, which facilitates stress transfer between surrounding wood cells via their pits, and the enhanced stress transfer through mechanically interlocked fiber-fiber interfaces, the reported stiffness values significantly exceed the upper limit of the rule of mixtures. Using this innovative technique, high-performance, sustainable materials that can substitute glass fibre reinforced composites or natural fibre composites can be produced with minimal environmental impact and at a low cost.

Using a similar principle, delignification and densifying the flax can improve the FVC and could ultimately;e improve the mechanical properties of the Flax/TPU composite.

References

[1] Amzan Alsabri, Furqan Tahir, and Sami G. Al-Ghamdi. "Life-Cycle Assessment of Polypropylene Production in the Gulf Cooperation Council (GCC) Region". In: *Polymers* 13.21 (2021). ISSN: 2073-4360. DOI: 10.3390/polym13213793. URL: https://www.mdpi.com/2073-4360/13/21/3793.

[2] Niklas von der Assen and AndrÃ© Bardow. "Life cycle assessment of polyols for polyurethane production using CO 2 as feedstock: Insights from an industrial case study". In: *Green Chemistry* 16 (Apr. 2014), pp. 3272–3280. DOI: 10.1039/C4GC00513A.

[3] Jens Bachmann, Carme Hidalgo, and StÃ©phanie Bricout. "Environmental analysis of innovative sustainable composites with potential use in aviation sectorâ€"A life cycle assessment review". In: *Science China Technological Sciences* 60.9 (Sept. 2017), pp. 1301–1317. ISSN: 1869-1900. DOI: 10.1007/s11431-016-9094-y. URL: https://doi.org/10.1007/s11431-016-9094-y.

[4] P.M Berry et al. "Understanding and Reducing Lodging in Cereals". In: Advances in Agronomy 84 (2004), pp. 217–271. ISSN: 0065-2113. DOI: https://doi.org/10.1016/S0065-2113(04)84005-7. URL: https://www.sciencedirect.com/science/article/pii/S0065211304840057.

[5] Francisco GarcÃa Calvo-Flores and JosÃ© A. Dobado. "Lignin as Renewable Raw Material". In: *ChemSusChem* 3.11 (2010), pp. 1227–1235. DOI: https://doi.org/10.1002/cssc.201000157. eprint: https://chemistry-europe.onlinelibrary.wiley.com/doi/pdf/10.1002/cssc.201000157. URL: https://chemistry-europe.onlinelibrary.wiley.com/doi/abs/10.1002/cssc.201000157.

[6] Leticia PeÃ±a Carrodeguas et al. "High elasticity, chemically recyclable, thermoplastics from bio-based monomers: carbon dioxide, limonene oxide and Îµ-decalactone". In: *Green Chem.* 22 (23 2020), pp. 8298–8307. DOI: 10.1039/D0GC02295K. URL: http://dx.doi.org/10.1039/D0GC02295K.

[7] Marla Carus. *Wood-plastic composites (WPC) and Natural Fibre Composites (NFC): European and global markets 2012 and future trends in automotive and construction*. 2015. URL: https://renewable-carbon.eu/publications/product/wood-plastic-composites-wpc-and-natural-fibre-composites-nfc-european-and-global-markets-2012-and-future-trends-in-automotive-and-construction/.

[8] Jonathon Chard et al. "Shades of Green: Life Cycle Assessment of a Urethane Methacrylate/Unsaturated Polyester Resin System for Composite Materials". In: *Sustainability* 11 (Feb. 2019), p. 1001. DOI: 10.3390/su11041001.

[9] Shikha Dahiya et al. "Biobased Products and Life Cycle Assessment in the Context of Circular Economy and Sustainability". In: *Materials Circular Economy* 2.1 (Sept. 2020), p. 7. ISSN: 2524-8154. DOI: 10.1007/s42824-020-00007-x. URL: https://doi.org/10.1007/s42824-020-00007-x.

[10] Joost R. Duflou et al. "Comparative impact assessment for flax fibre versus conventional glass fibre reinforced composites: Are bio-based reinforcement materials the way to go?" In: *CIRP Annals* 63.1 (2014), pp. 45–48. ISSN: 0007-8506. DOI: https://doi.org/10.1016/j.cirp.2014.03.061. URL: https://www.sciencedirect.com/science/article/pii/S000785061400064X.

[11] M Frey et al. "Delignified Woodâ€"Polymer Interpenetrating Composites Exceeding the Rule of Mixtures". In: *ACS Applied Materials Interfaces* 11 (38 Sept. 2019). doi: 10.1021/acsami.9b11105, pp. 35305–35311. ISSN: 1944-8244. DOI: 10.1021/acsami.9b11105. URL: https://doi.org/10.1021/acsami.9b11105.

[12] Anda Fridrihsone et al. "Life Cycle Assessment of vegetable oil based polyols for polyurethane production". In: *Journal of Cleaner Production* 266 (2020), p. 121403. ISSN: 0959-6526. DOI: https://doi.org/10.1016/j.jclepro.2020.121403. URL: https://www.sciencedirect.com/science/article/pii/S0959652620314505.

[13] SK Garkhail, RWH Heijenrath, and T Peijs. "Mechanical properties of natural-fibre-mat-reinforced thermoplastics based on flax fibres and polypropylene". In: *Applied Composite Materials* 7.5 (2000), pp. 351–372.

[14] Wim J. Groot and Tobias BorÃ©n. "Life cycle assessment of the manufacture of lactide and PLA biopolymers from sugarcane in Thailand". In: *The International Journal of Life Cycle Assessment* 15.9 (Nov. 2010), pp. 970–984. ISSN: 1614-7502. DOI: 10.1007/s11367-010-0225-y. URL: https://doi.org/10.1007/s11367-010-0225-y.

[15] Charles Guy et al. "Metabolomics of temperature stress". In: *Physiologia Plantarum* 132.2 (2008), pp. 220–235. DOI: https://doi.org/10.1111/j.1399-3054.2007.00999.x. eprint: https://onlinelibrary.wiley.com/doi/pdf/10.1111/j.1399-3054.2007.00999.x. URL: https://onlinelibrary.wiley.com/doi/abs/10.1111/j.1399-3054.2007.00999.x.

[16] Mei-po Ho et al. "Critical factors on manufacturing processes of natural fibre composites". In: *Composites Part B: Engineering* 43.8 (2012), pp. 3549–3562. ISSN: 1359-8368. DOI: https://doi.org/10.1016/j.compositesb.2011.10.001. URL: https://www.sciencedirect.com/science/article/pii/S1359836811004483.

[17] Wieland Hoppe, Nils Thonemann, and Stefan Bringezu. "Life Cycle Assessment of Carbon Dioxideâ€"Based Production of Methane and Methanol and Derived Polymers". In: *Journal of Industrial Ecology* 22.2 (2018), pp. 327–340. DOI: https://doi.org/10.1111/jiec.12583. eprint: https://onlinelibrary.wiley.com/doi/pdf/10.1111/jiec.12583. URL: https://onlinelibrary.wiley.com/doi/abs/10.1111/jiec.12583.

[18] Troy A. Hottle, Melissa M. Bilec, and Amy E. Landis. "Sustainability assessments of bio-based polymers". In: *Polymer Degradation and Stability* 98.9 (2013), pp. 1898–1907. ISSN: 0141-3910. DOI: https://doi.org/10.1016/j.polymdegradstab.2013.06.016. URL: https://www.sciencedirect.com/science/article/pii/S0141391013001870.

[19] "Chapter 1 - Introduction". In: *Lignin Chemistry and Applications*. Ed. by Jin Huang, Shiyu Fu, and Lin Gan. Elsevier, 2019, pp. 1–24. ISBN: 978-0-12-813941-7. DOI: https://doi.org/10.1016/B978-0-12-813941-7.00001-1. URL: https://www.sciencedirect.com/science/article/pii/B9780128139417000011.

[20] Umit Huner. "Effect of Chemical Surface Treatment on Flax-Reinforced Epoxy Composite". In: *Journal of Natural Fibers* 15 (6 2018), pp. 808–821. DOI: 10.1080/15440478.2017.1369207. URL: https://doi.org/10.1080/15440478.2017.1369207.

[21] Panatda Jannoey et al. "Expression Analysis of Genes Related to Rice Resistance Against Brown Planthopper, Nilaparvata lugens". In: *Rice Science* 24.3 (2017), pp. 163–172. ISSN: 1672-6308. DOI: https://doi.org/10.1016/j.rsci.2016.10.001. URL: https://www.sciencedirect.com/science/article/pii/S1672630817300215.

[22] Y.K. Kim. "8 - Natural fibre composites (NFCs) for construction and automotive industries". In: Woodhead Publishing Series in Textiles 2 (2012). Ed. by Ryszard M. Koz?owski, pp. 254–279. DOI: https://doi.org/10.1533/9780857095510.2.254. URL: https://www.sciencedirect.com/science/article/pii/B9781845696986500085.

[23] Angela Daniela La Rosa et al. "Bio-based versus traditional polymer composites. A life cycle assessment perspective". In: *Journal of Cleaner Production* 74 (2014), pp. 135–144. ISSN: 0959-6526. DOI: https://doi.org/10.1016/j.jclepro.2014.03.017. URL: https://www.sciencedirect.com/science/article/pii/S0959652614002388.

[24] Antoine Le Duigou and Christophe Baley. "Coupled micromechanical analysis and life cycle assessment as an integrated tool for natural fibre composites development". In: *Journal of Cleaner Production* 83 (2014), pp. 61–69. ISSN: 0959-6526. DOI: https://doi.org/10.1016/j.jclepro.2014.07.027. URL: https://www.sciencedirect.com/science/article/pii/S095965261400732X.

[25] Qingquan Liu, Le Luo, and Luqing Zheng. "Lignins: Biosynthesis and Biological Functions in Plants". In: *International Journal of Molecular Sciences* 19.2 (2018). ISSN: 1422-0067. DOI: 10.3390/ijms19020335. URL: https://www.mdpi.com/1422-0067/19/2/335.

[26] Zhengyi Liu et al. "Research on mechanical properties and durability of flax/glass fiber bio-hybrid FRP composites laminates". In: *Composite Structures* 290 (2022), p. 115566. ISSN: 0263-8223. DOI: https://doi.org/10.1016/j.compstruct.2022.115566. URL: https://www.sciencedirect.com/science/article/pii/S0263822322003531.

[27] Marc Li Loong and Duncan Cree. "Enhancement of Mechanical Properties of Bio-Resin Epoxy/Flax Fiber Composites using Acetic Anhydride". In: *Journal of Polymers and the Environment* 26.1 (Jan. 2018), pp. 224–234. ISSN: 1572-8900. DOI: 10.1007/s10924-017-0943-3. URL: https://doi.org/10.1007/s10924-017-0943-3.

[28] Maria Morissa Lu, Carlos A. Fuentes, and Aart Willem Van Vuure. "Moisture sorption and swelling of flax fibre and flax fibre composites". In: *Composites Part B: Engineering* 231 (2022), p. 109538. ISSN: 1359-8368. DOI: https://doi.org/10.1016/j.compositesb.2021.109538. URL: https://www.sciencedirect.com/science/article/pii/S1359836821009045.

[29] Mahmoud Yousry Mahmoud Zaghloul, Moustafa Mahmoud Yousry Zaghloul, and Mai Mahmoud Yousry Zaghloul. "Developments in polyester composite materials â€" An in-depth review on natural fibres and nano fillers". In: *Composite Structures* 278 (2021), p. 114698. ISSN: 0263-8223. DOI: https://doi.org/10.1016/j.compstruct.2021.114698. URL: https://www.sciencedirect.com/science/article/pii/S0263822321011533.

[30] Menghe MIAO and Niall FINN. "Conversion of Natural Fibres into Structural Composites". In: *Journal of Textile Engineering* 54.6 (2008), pp. 165–177. DOI: 10.4188/jte.54.165.

[31] Kush Kumar Nayak, Piyush Parkhey, and Reecha Sahu. "Analysis of Lignin Using Qualitative and Quantitative Methods". In: *Lignin: Biosynthesis and Transformation for Industrial Applications*. Ed. by Swati Sharma and Ashok Kumar. Cham: Springer International Publishing, 2020, pp. 115–138. ISBN: 978-3-030-40663-9. DOI: 10.1007/978-3-030-40663-9_4. URL: https://doi.org/10.1007/978-3-030-40663-9_4.

[32] Faris M. AL-Oqla and Mohd S. Salit. "2 - Natural fiber composites". In: (2017). Ed. by Faris M. AL-Oqla and Mohd S. Salit, pp. 23–48. DOI: https://doi.org/10.1016/B978-0-08-100958-1.00002-5. URL: https://www.sciencedirect.com/science/article/pii/B9780081009581000025.

[33] Paulo PeÃ§as et al. "Natural Fibre Composites and Their Applications: A Review". In: *Journal of Composites Science* 2.4 (2018). ISSN: 2504-477X. DOI: 10.3390/jcs2040066. URL: https://www.mdpi.com/2504-477X/2/4/66.

[34] Muhammad Pervaiz and Mohini M Sain. "Carbon storage potential in natural fiber composites". In: *Resources, Conservation and Recycling* 39 (4 2003), pp. 325–340. ISSN: 0921-3449. DOI: https://doi.org/10.1016/S0921-3449(02)00173-8. URL: https://www.sciencedirect.com/science/article/pii/S0921344902001738.

[35] Thien An Phung Hai et al. "Flexible polyurethanes, renewable fuels, and flavorings from a microalgae oil waste stream". In: *Green Chem.* 22 (10 2020), pp. 3088–3094. DOI: 10.1039/D0GC00852D. URL: http://dx.doi.org/10.1039/D0GC00852D.

[36] Thien An Phung Hai et al. "Preparation of Mono- and Diisocyanates in Flow from Renewable Carboxylic Acids". In: *Organic Process Research & Development* 24.10 (2020), pp. 2342–2346. DOI: 10.1021/acs.oprd.0c00167. eprint: https://doi.org/10.1021/acs.oprd.0c00167. URL: https://doi.org/10.1021/acs.oprd.0c00167.

[37] Thien An Phung Hai et al. "Renewable Polyurethanes from Sustainable Biological Precursors". In: *Biomacromolecules* 22.5 (2021). PMID: 33822601, pp. 1770–1794. DOI: 10.1021/acs.biomac.0c01610. eprint: https://doi.org/10.1021/acs.biomac.0c01610. URL: https://doi.org/10.1021/acs.biomac.0c01610.

[38] Emily Preedy. *USING ALGAE TO CLEAN UP INDUSTRY EMISSIONS*. 2020. URL: https://www.swansea.ac.uk/research/research-highlights/sustainable-futures-energy-environment/algae/#:~:text=As%5C%20trees%5C%20and%5C%20plants%5C%20can,per%5C%20kilogram%5C%20of%5C%20algal%5C%20biomass..

[39] Daniel Steeg. *Carbon footprint and sustainability of different natural fibres for biocomposites and insulation material full version (update 2019)*. 2019. URL: https://renewable-carbon.eu/publications/product/carbon-footprint-and-sustainability-of-different-natural-fibres-for-biocomposites-and-insulation-material-%5C%e2%5C%88%5C%92-full-version-update-2019/.

[40] B van Voorn et al. "Natural fibre reinforced sheet moulding compound". In: *Composites Part A: Applied Science and Manufacturing* 32 (9 2001), pp. 1271–1279. ISSN: 1359-835X. DOI: https://doi.org/10.1016/S1359-835X(01)00085-9. URL: https://www.sciencedirect.com/science/article/pii/S1359835X01000859.

[41] W. Woigk et al. "Interface properties and their effect on the mechanical performance of flax fibre thermoplastic composites". In: *Composites Part A: Applied Science and Manufacturing* 122 (2019), pp. 8–17. ISSN: 1359-835X. DOI: https://doi.org/10.1016/j.compositesa.2019.04.015. URL: https://www.sciencedirect.com/science/article/pii/S1359835X19301435.

[42] Libo Yan, Nawawi Chouw, and Krishnan Jayaraman. "Flax fibre and its composites â€" A review". In: *Composites Part B: Engineering* 56 (2014), pp. 296–317. ISSN: 1359-8368. DOI: https://doi.org/10.1016/j.compositesb.2013.08.014. URL: https://www.sciencedirect.com/science/article/pii/S1359836813004228.

[43] Mengjing Zheng et al. "Manipulation of lignin metabolism by plant densities and its relationship with lodging resistance in wheat". In: *Scientific Reports* 7.1 (Feb. 2017), p. 41805. ISSN: 2045-2322. DOI: 10.1038/srep41805. URL: https://doi.org/10.1038/srep41805.